CHALMERS
UNIVERSITY OF TECHNOLOGY

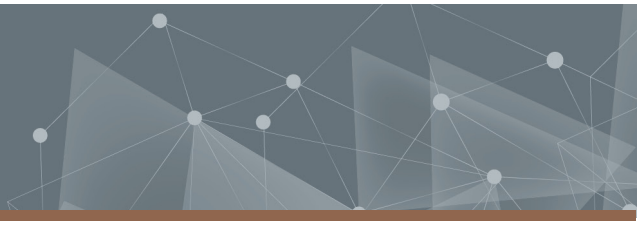

# Equivalent circuit parameter estimation of an induction machine using finite element analysis

DIMITRIOS SAGRIS

DEPARTMENT OF ELECTRICAL ENGINEERING

CHALMERS UNIVERSITY OF TECHNOLOGY
Gothenburg, Sweden 2021
www.chalmers.se

Master's thesis 2021

# Equivalent circuit parameter estimation of an induction machine using finite element analysis

DIMITRIOS SAGRIS


CHALMERS
UNIVERSITY OF TECHNOLOGY

Department of Electrical Engineering
*Division of Electric Power Engineering*
Chalmers University of Technology
Gothenburg, Sweden 2021

Equivalent circuit parameter estimation of an induction machine using finite element analysis
DIMITRIOS SAGRIS



Supervisor: Torbjörn Thiringer, Department of Electrical Engineering
Examiner: Torbjörn Thiringer, Department of Electrical Engineering

Master's Thesis 2021
Department of Electrical Engineering
Division of Electric Power Engineering
Chalmers University of Technology
SE-412 96 Gothenburg
Telephone +46 31 772 1000

Typeset in LaTeX
Printed by Chalmers Reproservice
Gothenburg, Sweden 2021

Equivalent circuit parameter estimation of an induction machine using finite element analysis
DIMITRIOS SAGRIS
Department of Electrical Engineering
Chalmers University of Technology

# Abstract

In this project, finite element analysis has been conducted in order to estimate the parameters of an induction machine. A model of a 15kW induction machine in Ansys Maxwell was the main object of the investigation. Using the field analysis from Ansys and in combination with the Ansys result outputs, the stator leakage inductance and the rotor resistance were investigated. After that, a parameter estimation of the parameters in the $\tau$ model and in the ך was carried out.

The performed analysis showed that there can be a good estimation of the stator leakage inductance in the case of having a linear material in the core. Moreover, the estimation of the rotor resistance using the field analysis from Ansys gave a very close value compared to the theoretically calculated value of the rotor resistance (from geometrical data). Finally, considering the rotor resistance, the stator flux from Ansys result output and the stator current from Ansys result output, a parameter estimation process could be performed.



Keywords: induction machine, parameter calculation, finite element analysis.

# Acknowledgements

I would like to thank my supervisor and examiner, professor Torbjörn Thiringer, for the encouraging guidance and vital advice.

I would like to thank PhD student Meng-Ju Hsieh, for the nice cooperation.

Dimitrios Sagris, Gothenburg, June 2021

# Contents


**1 Introduction** **1**
- 1.1 Background . . . 1
- 1.2 Related work . . . 1
- 1.3 Scope . . . 1
- 1.4 Aim and layout of the thesis . . . 1

**2 Theoretical background** **3**
- 2.1 Induction machine theory . . . 3
- 2.2 Inductance and flux connection . . . 8
- 2.3 Parameter calculation . . . 9

**3 Case setup** **12**

**4 Analysis** **16**
- 4.1 Inductance investigation . . . 16
  - 4.1.1 Flux distribution . . . 16
  - 4.1.2 Finding Leakage Inductance . . . 25
  - 4.1.3 Adding saturation . . . 31
- 4.2 Power balance check . . . 37
- 4.3 Rotor resistance . . . 43
  - 4.3.1 Rotor resistance from locked rotor test . . . 44
  - 4.3.2 Rotor resistance from field analysis . . . 48
- 4.4 Stator leakage inductance . . . 51
- 4.5 Parameter estimation . . . 52
  - 4.5.1 Processing the data . . . 52
  - 4.5.2 Results at load test . . . 54
- 4.6 Sustainable aspects . . . 57

**5 Conclusion and future work** **58**
- 5.1 Conclusion . . . 58
- 5.2 Future work . . . 59

# 1
# Introduction

## 1.1 Background

Identifying the parameters of an induction machine is crucial for the design of an effective controller. The temperature variations affect the conductivity of a material. The magnetic field can affect the permeability of a material. This is one reason why the leakage and magnetization inductance of an induction machine are not constant during different operation points.

## 1.2 Related work

Some models of parameter identification considering magnetic saturation have been found in literature where different methods in order to achieve inductance estimation have been described. In [1] the use of cost function is combined with inductance estimation. In [12] an iteration process is described in order to estimate the leakage and magnetizing inductance. In [2] the magnetizing inductance is expressed considering a constant leakage inductance.

## 1.3 Scope

All investigations were made using finite element analysis. A 15kW induction machine using a squired cage rotor was simulated in Ansys Maxwell.

## 1.4 Aim and layout of the thesis

The purpose of this project is to investigate the parameter estimation of an induction machine using finite element analysis.

In chapter 4.1 the outputs of the inductance matrix from Ansys Maxwell are investigated. In chapter 4.2 the power balance is examined and a manual calculation of the torque is described. In chapter 4.3 the rotor resistance is estimated with two different approaches. In chapter 4.4 the stator leakage inductance is approximated. In chapter 4.5 a parameter investigation is described from load test simulations.

# 2

# Theoretical background

## 2.1 Induction machine theory

In this thesis work an induction machine using a squired cage rotor is examined in steady state. Equations of the $\tau$ model and equations of the $\urcorner$ model are used in steady state. More models of the induction machine can be found in [2].

#### Induction machine in xy coordinates, $\tau$ model

In a rotating system (xy coordinates) and with a speed of $\omega_1$ the equations of the stator voltage, rotor voltage, stator flux, rotor flux and electromagnetic torque are

$$u_s = R_s i_s + \frac{d\psi_s}{dt} + j\omega_1 \psi_s \tag{2.1}$$

$$u_r = R_r i_r + \frac{d\psi_r}{dt} + j(\omega_1 - \omega_r)\psi_r \tag{2.2}$$

$$\psi_s = L_s i_s + L_m i_r \tag{2.3}$$

$$\psi_r = L_r i_r + L_m i_s \tag{2.4}$$

$$T_e = \frac{3n_p}{2}(\psi_{sx} i_{sy} - \psi_{sy} i_{sx}) \tag{2.5}$$

where
$u_s$ stator voltage in xy coordinates
$i_s$ stator current in xy coordinates
$R_s$ stator resistance
$R_r$ rotor resistance
$\psi_s$ stator flux
$\psi_r$ rotor flux
$\omega_1$ synchronous electrical rotation speed
$\omega_r$ rotor electrical rotation speed
$L_s$ self inductance of the stator
$L_r$ self inductance of the rotor
$L_m$ mutual inductance between stator and rotor
$T_e$ electromagnetic torque

### IM in xy coordinates, ⅂ model

Introducing $b$ as an important ratio constant,

$$b = \frac{L_m}{L_r} \tag{2.6}$$

and according to [7] the units of the rotor flux and rotor current in the ⅂ model can be related as

$$\Psi_R = b\psi_r \tag{2.7}$$

$$i_R = \frac{i_r}{b} \tag{2.8}$$

The magnetization inductance and leakage inductance in the ⅂ model can expressed as

$$L_M = \frac{L_m^2}{L_r} \tag{2.9}$$

$$L_\sigma = L_s - L_M \tag{2.10}$$

and the rotor resistance in the ⅂ model is

$$R_R = b^2 R_r \tag{2.11}$$

while the stator flux and the rotor flux in the ⅂ model can expressed as

$$\psi_s = (L_\sigma + L_M)i_s + L_M i_R \tag{2.12}$$

$$\psi_R = L_M i_s + L_M i_R \tag{2.13}$$

where
$L_r$ self inductance of the rotor
$\Psi_R$ rotor flux in the ⅂ model
$i_R$ rotor current in the ⅂ model
$L_M$ magnetization inductance
$L_\sigma$ leakage inductance in the ⅂ model

From (2.12) and (2.13), the stator flux and rotor current can be expressed also as

$$\psi_s = L_\sigma i_s + \Psi_R \tag{2.14}$$

$$i_R = \frac{\Psi_R - L_M i_s}{L_M} \tag{2.15}$$

Now the equations of the stator voltage, rotor voltage and torque become

$$u_s = R_s i_s + \frac{d\psi_s}{dt} + j\omega_1 \psi_s \tag{2.16}$$

$$u_r = 0 = R_R i_R + \frac{d\Psi_R}{dt} + j(\omega_1 - \omega_r)\Psi_R \tag{2.17}$$

$$T_e = \frac{3n_p}{2} \Im \psi_s^* i_s \tag{2.18}$$

$$T_e = \frac{3n_p}{2} (\Psi_{Rd} i_{sq} - \Psi_{Rq} i_{sd}) \tag{2.19}$$

In dq coordinates the rotor flux is

$$\Psi_R = \Re \Psi_R = \Psi_{Rd} \tag{2.20}$$

Combining (2.14), (2.15), (2.16) and (2.17) the stator voltage becomes

$$us = L_\sigma \frac{di_s}{dt} + (R_s + R_R + j\omega_1 L\sigma) i_s + (j\omega_r - \frac{R_R}{L_M})\Psi_R \tag{2.21}$$

while from the rotor voltage equation the following relation is obtained

$$\frac{d\Psi_R}{dt} = R_R i_s - (\frac{R_R}{L_M} + j(\omega_1 - \omega_r))\Psi_R \tag{2.22}$$

and the electromagnetic torque can expressed as

$$T_e = \frac{3n_p}{2} (\Psi_R i_q) \tag{2.23}$$

If steady state is considered then the derivatives of the stator and rotor flux are

$$\frac{d\psi_s}{dt} = 0 \tag{2.24}$$

$$\frac{d\Psi_R}{dt} = 0 \tag{2.25}$$

then taking the real part of (2.22)

$$R_R i_{sd} = \Psi_R \frac{R_R}{L_M} \tag{2.26}$$

$$\Psi_R = i_{sd} L_M \tag{2.27}$$

and taking the imaginary part of (2.22), we find

$$\omega_{slip} = (\omega_1 - \omega_r) = \frac{R_R i_{sq}}{\Psi_R} \tag{2.28}$$

where
$\omega_{slip}$ angular velocity of the slip frequency

Considering (2.28) and (2.23), torque can be expressed as

$$T_e = \frac{3n_p}{2} \frac{R_R i_q^2}{w_{slip}} \tag{2.29}$$

**Losses**

The induction machine in this paper is examined without taking into account mechanical friction. The windings of the machine are made of copper and the rotor bars are made of aluminium. The total losses considering only electromagnetic analysis will be

$$P_{totallosses} = P_{cu} + P_{solid} + Pfe \tag{2.30}$$

where copper looses are

$$P_{cu} = \sqrt{3} I_{sRMS}^2 R_s \tag{2.31}$$

and solid losses are

$$P_{solid} = \sqrt{3} I_{rRMS}^2 R_r \tag{2.32}$$

where
$P_{cu}$ total copper losses of the stator windings
$P_{fe}$ total iron losses
$P_{solid}$ total losses of the rotor bars
$I_{sRMS}$ RMS value of stator current
$I_{rRMS}$ RMS value of the equivalent in stator side rotor current

Iron losses can be expressed with different models as explained in [4]. One model is the separation of iron losses in hysteresis based losses ($P_{hys}$) and eddy current based losses ($P_{eddy}$).

$$P_{fe} = P_{hys} + P_{eddy} \tag{2.33}$$

According to [4] (2.33) lacks accuracy for Si-Fe alloys and a third component in the iron losses can be added called excess losses. Iron losses can be re-expressed as

$$P_{fe} = P_{hys} + P_{eddy} + P_{excess} \tag{2.34}$$

where
$P_{excess}$ is the excess losses

Losses can be divided to more categories which can be found in [8].

### Power balance

Power balance should be satisfied, which means that the input electrical power should be equal to the output power. The output power is comprised by the mechanical power and the losses of the machine

$$P_{in} = P_{out} \tag{2.35}$$

$$u_a i_a + u_b i_b + u_c i_c = T\Omega_r + P_{totallosses} \tag{2.36}$$

where
$P_{in}$ total input electrical power
$P_{out}$ total output power
$T$ output Torque
$u_a$ voltage of phase $a$
$u_b$ voltage of phase $b$
$u_c$ voltage of phase $c$
$i_a$ current of phase $a$
$i_b$ current of phase $b$
$i_c$ current of phase $c$
$\Omega_r$ mechanical speed of the rotor

## 2.2 Inductance and flux connection

The flux linkage of phase $a$ caused by the influence of the 3 stator currents $i_{sa}$, $i_{sb}$ and $i_{sc}$ is given by

$$\Psi_{sa} = (L_{s\sigma} + L_h)i_{sa} + M_{ab}i_{sb} + M_{ac}i_{sc} \tag{2.37}$$

where
$\Psi_{sa}$ the flux of phase $a$
$L_{s\sigma}$ stator leakage inductance
$L_h$ main inductance of a single phase
$M_{ab}$ mutual inductance between phase a and b
$M_{ac}$ mutual inductance between phase a and c

In case of a star connection the summation of the three stator currents is zero

$$i_{sa} + i_{sb} + i_{sc} = 0 \tag{2.38}$$

If the mutual inductances are equal, then

$$M_{ab} = M_{ac} \tag{2.39}$$

Combing (2.38) and (2.39), equation (2.37) becomes

$$\Psi_{sa} = (L_{s\sigma} + L_h)i_{sa} + Mi_{sa} \tag{2.40}$$

The stator flux of the phase $a$ can be also expressed as

$$\Psi_{sa} = L_s i_{sa} \tag{2.41}$$

where $L_s$ is the self inductance

$M$ and $L_h$ are connected with an angle $\theta$ as

$$M = L_h cos\theta \tag{2.42}$$

where $\theta$ is the angle between 2 phase windings.

## 2.3 Parameter calculation

**Stator resistance**

The resistivity of copper can be expressed as

$$\rho_{Cu} = 16.8 \cdot 10^{-9} \cdot (1 + 3.9 \cdot 10^{-3} \cdot (T_{cu} - 20)) \tag{2.43}$$

where
$T_{cu}$ temperature of the copper in Celsius

The resistance of the active winding is

$$Rs_{aw} = \frac{\rho_{Cu} \cdot L_{AW} \cdot n_s q_s}{A_{cu} \cdot c_s \cdot n_{strands}} \tag{2.44}$$

where
$\rho_{Cu}$ is the resistivity of copper
$L_{AW}$ is the length of the active winding
$n_s$ is the number of turns per coil
$q_s$ is the number of slots per phase per pole pair
$A_{cu}$ is the area of the copper conductor
$c_s$ is the winding factor which depends on the way the phases are connected and the parallel branches
$n_{strands}$ is the number of strands

The resistance of the end winding is

$$Rs_{ew} = \frac{\rho_{Cu} \cdot L_{EW} \cdot n_s \cdot q_s}{A_{cu} c_s \cdot n_{strands}} \tag{2.45}$$

where
$L_{EW}$ is the length of the end winding

The total stator resistance is comprised of the resistance of the active winding and the resistance of the end winding

$$R_s = Rs_{aw} + Rs_{ew} \tag{2.46}$$

It should be noted that in this project the simulations are been carried out in 2D simulation using FEA and the end winding resistance is not contributing to the stator resistance.

### Rotor resistance

The resistivity of the rotor bar in case of aluminium material can be expressed as

$$\rho_{al} = 28.2 \cdot 10^{-9} \cdot (1 + 4.3 \cdot 10^{-3} \cdot (T_{al} - 20)) \tag{2.47}$$

where
$T_{al}$ is the temperature of the aluminium in Celcius

The resistance of a single bar is

$$R_{bar} = \rho_{al} L_a / A_{bar} \tag{2.48}$$

where
$L_a$ is the length of the bar
$A_{bar}$ is the cross section of the bar in the case of current in z direction

The resistance of the end ring is

$$R_{endring} = (2\pi \cdot \rho_{al} \cdot r_{scr})/(Q_r \cdot A_{scr}) \tag{2.49}$$

where
$A_{scr}$ can be expressed according to [5] as

$$A_{scr} = \frac{Q_r A_{bar}}{\pi poles} \tag{2.50}$$

where
$Q_r$ is the number of total bars
$poles$ is the number of total poles
$r_{scr}$ is the mean radius of the end ring

Expressing the rotor units to stator equivalent units, the coefficients for this conversion are obtained. The coefficient to convert the rotor current to stator equivalent rotor current is

$$coef_{reqS} = \frac{3 n_s^2 q_s^2 k_1^2 poles^2}{Q_r c_s^2} \tag{2.51}$$

and the coefficient to convert the rotor resistance to stator equivalent rotor resistance is

$$coef_{ieqS} = \frac{Q_r c_s}{3 n_s q_s k_1 poles} \tag{2.52}$$

where
$k_1$ is the harmonic winding factor

$coef_{reqS}$ is the coefficient to connect the rotor equivalent resistance to stator equivalent
$coef_{ieqS}$ is the coefficient to connect the rotor equivalent current to stator equivalent

The stator equivalent resistance of the end ring is

$$Rr_{endring} = \frac{coef_{reqS} \cdot 2 \cdot R_{endring} \cdot Q_r}{(\pi \cdot poles)^2} \tag{2.53}$$

The stator equivalent rotor bar resistance is

$$Rr_{bar} = coef_{reqS} R_{bar} \tag{2.54}$$

The total rotor resistance of the rotor in the stator side can be expressed as

$$R_r = Rr_{bar} + Rr_{endring} \tag{2.55}$$

# 3

# Case setup

In this project all investigations were made using finite element analysis. A 15kW induction machine using a squired cage rotor was simulated in Ansys Maxwell which was the main object of investigation. However, some more modified versions were made in order to investigate inductances as described in chapter 4.

**Induction Machine 15kW**

Table 3.1 shows the parameters of the stator geometry. Table 3.2 shows the parameters of the rotor geometry. Figure 3.1 shows the position of the geometrical parameters in the stator and rotor slot.

The number of turns per coil are 38 and a single layer of winding is modeled per stator slot. One winding per pole pair is comprised by 2 coils connected in series. The total number of parallel branches per phase are 3. All three windings had a star connection with each other. No end ring is modeled in the model.

Stator windings are made of copper and rotor bars are made of aluminum. M700 is the non-linear material of the core. Table 3.3 shows the basic characteristics of these three materials. Table 3.4 shows the points of the B-H curve of M700.

It should be noted that iron losses exist in the core material. However, the simulation settings are modified in a way that iron losses do not affect the field solutions of Ansys Maxwell.

**Table 3.1:** Stator geometry

| Name | Value | Description |
|---|---|---|
| SOD | 291.2mm | Stator outer dimameter |
| SID | 190.2mm | Stator inner diameter |
| slots | 36 | Number of stator slots |
| HSO | 1mm | Slot opening heght |
| HSO1 | 0 | Slot closed bridge heght |
| HS1 | 1mm | Slot wedge heght |
| HS2 | 13.5mm | Slot body heght |
| BSO | 3.5mm | Slot opening width |
| BS1 | 8.5mm | Slot wedge maximum width |
| BS2 | 11mm | Slot body bottom width, 0 for parallel teeth |
| Rs | 2mm | Slot body bottom fillet |

**Table 3.2:** Rotor goemetry

| Name | Value | Description |
|---|---|---|
| ROD | 189.3mm | Rotor outer dimameter |
| RID | 55mm | Rotor inner diameter |
| slots | 39 | Number of rotor bars |
| HSO | 8mm | Slot opening heght |
| HSO1 | 0 | Slot closed bridge heght |
| HS1 | 0.2mm | Slot wedge heght |
| HS2 | 9.7mm | Slot body heght |
| BSO | 3.35mm | Slot opening width |
| BS1 | 5.9mm | Slot wedge maximum width |
| BS2 | 3.9mm | Slot body bottom width, 0 for parallel teeth |
| Rs | 0.3mm | Slot body bottom fillet |

**Table 3.3:** Materials used for IM

| Material | Conductivity (S/m) | Relative permebility |
|---|---|---|
| Copper | 57350900 | 1 |
| Aluminium | 33055600 | 1 |
| M700 | 0 | B-H curve |

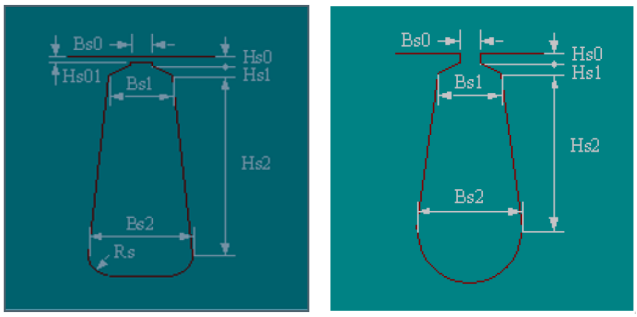


**Figure 3.1:** Example of a stotor slot(left) and a rotor slot(right)

**Table 3.4:** Points for the B-H curve of M700

| H (A/m) | B (T) |
|---|---|
| 0 | 0 |
| 67.8 | 0.1 |
| 88.3 | 0.2 |
| 99.2 | 0.3 |
| 108 | 0.4 |
| 116 | 0.5 |
| 124 | 0.6 |
| 132 | 0.7 |
| 142 | 0.8 |
| 152 | 0.9 |
| 164 | 1 |
| 180 | 1.1 |
| 206 | 1.2 |
| 254 | 1.3 |
| 363 | 1.4 |
| 690 | 1.5 |
| 1760 | 1.6 |
| 4230 | 1.7 |
| 8130 | 1.8 |
| 8239 | 1.802 |
| 8571 | 1.81 |
| 9137 | 1.82 |
| 9955 | 1.83 |
| 11060 | 1.85 |
| 12504 | 1.86 |
| 14381 | 1.875 |
| 16878 | 1.887 |
| 20467 | 1.899 |
| 30000 | 1.9193 |
| 150000 | 3.8 |

Figure 3.2 shows the model of the induction machine in Ansy Maxwell. Some times the induction machine was excited with voltage excitation and some times with current excitation.

When current excitation was applied a typical simulation was set to last 1 second. When voltage excitation was applied a typical simulation was set to last 0.5 seconds.

A simulation with voltage excitation typically reaches steady state after 0.4 seconds. One extra resistance was added (in voltage excitation case) in order to damp the high initial currents. Figure 3.3 shows how this extra resistance looks in time.

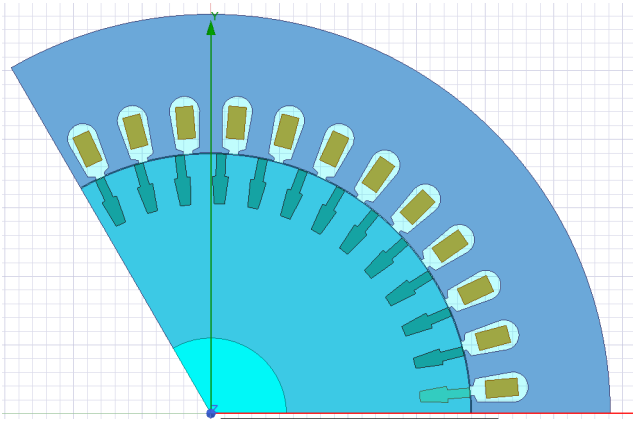

**Figure 3.2:** IM main model

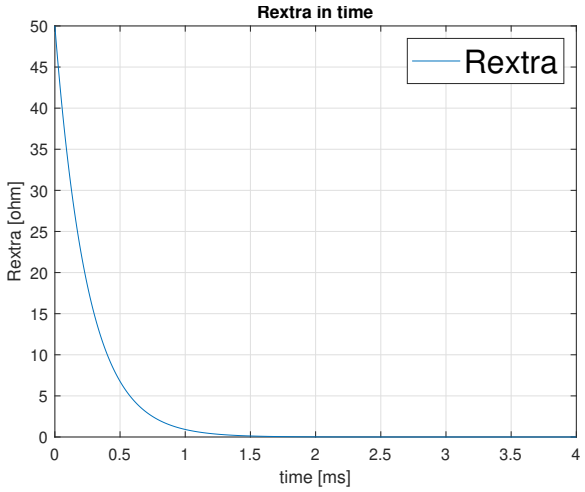


**Figure 3.3:** Extra resistance added as an additional stator resistance

# 4

# Analysis

## 4.1 Inductance investigation

Some efforts have been made in order to calculate stator inductances from the Ansys simulations. It should be mentioned that Ansys Maxwell provides an inductance matrix calculation option which is used in the simulations. However, it is unclear what the results from the Ansys inductance matrix calculation stand for and how useful these results are for our investigation.

### 4.1.1 Flux distribution

In this part flux distribution will be examined. First, it is desired to eliminate leakage flux and try to make the flux distribution homogeneous. In order to achieve the first one, the slot opening is made from an unreal material with $\mu$r of 0.0001. In order to achieve the second one, the slot opening is modified as shown in the Figure 4.1 and the core material is replaced by a steel with constant relative permeability of 10000. Moreover, the rotor bars are made of the new core material for this initial study.

A modified geometry as shown in the Figure 4.3 is tested with a DC current of 50A and no rotor speed. Table 4.1 shows the total flux given by Ansys result output, the main flux that comes from the field calculator and the flux through the slot opening that comes from the field calculator. Moreover, Table 4.1 shows two cases of slot material.

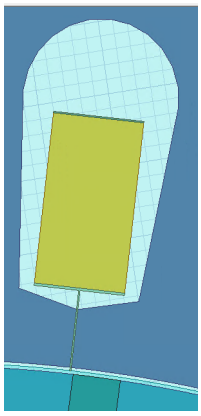

**Figure 4.1:** Modified slot opening, light green is the unreal material with $\mu r$ of 0.0001

The flux from the field analysis can be calculated from

$$\Psi_f = \iint_S B_{normal} dS \cdot N_{turnscoil} \tag{4.1}$$

where
$\Psi_f$ is the fundamental flux
$B_{normal}$ is the normal component of the flux density
$S$ is the coss section of the $B_{normal}$
$N_{turnscoil}$ is the number of turns per coil

The line of the stator surface is been taken according to Figure 4.2

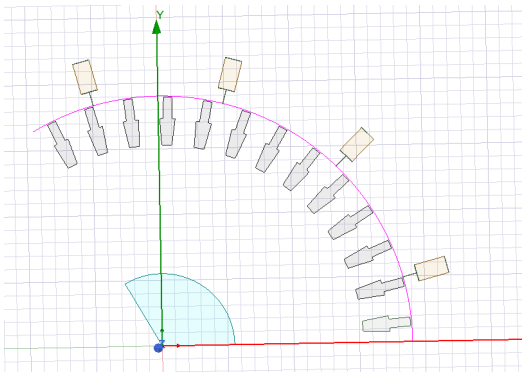

**Figure 4.2:** Line of stator surface

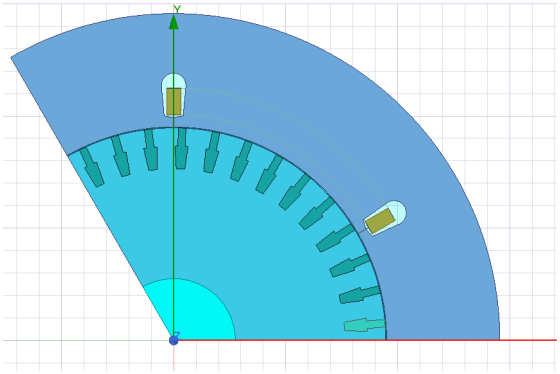

**Figure 4.3:** Modified geometry

**Table 4.1:** Total and main flux of the coil taken from Ansys result output and from Ansys field calculator

| Material of slot opening | Main flux coming from the Ansys field calculator (Wb) | Flux coming from the Ansys result output (Wb) | Flux through one slot opening (Wb) coming from the Ansys field calculator |
|---|---|---|---|
| $\mu r = 0.0001$<br>air | 1.108<br>1.102 | 1.108<br>1.882 | $5.6 \cdot 10^{-5}$<br>0.3935 |

Two more cases are examined with 2 different coils as shown in Figure 4.4 and Figure 4.5. In the first case, the coil occupies half of the total geometrical angle of the pole pair while in the second case the coil occupies 2/3 of the total geometrical angle of the pole pair. The total flux density inside the coil will be the same as the total flux density outside the coil

$$\int B_{normalin} dS = \int B_{normalout} dS \tag{4.2}$$

and in the case of homogeneous flux distribution the flux density is the same everywhere. Equation (4.2) will result to

$$B_{normalin} A_{crossin} = B_{normalout} A_{crossout} \tag{4.3}$$

where
$B_{normalin}$ is the normal flux density between the coil conductors
$B_{normalout}$ is the normal flux density outside the coil
$A_{crossin}$ is the cross section of the $B_{normalin}$
$A_{crossout}$ is the cross section of the $B_{normalout}$

In Figure 4.6 and Figure 4.7 are shown the $B_{normal}$ along the stator surface for the examined cases respectively. It is clear that when $A_{crossout}$ is smaller, then $B_{normalout}$ becomes bigger according to (4.3). The spots where $B_{normal}$ is reaching 0 quickly indicate the positions of the slot openings. One more visualization of the magnetic flux density vectors is shown in the Figure 4.8 for the second case only.

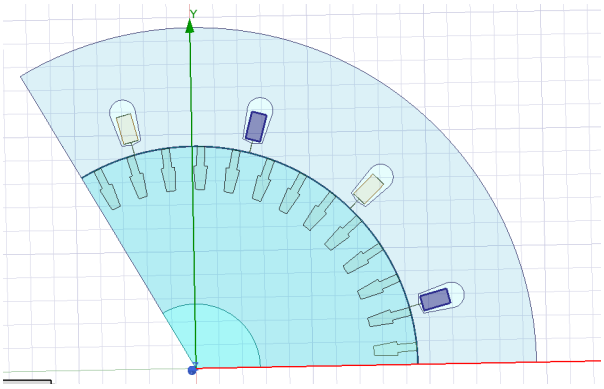

**Figure 4.4:** Position of the coil in the first examined case

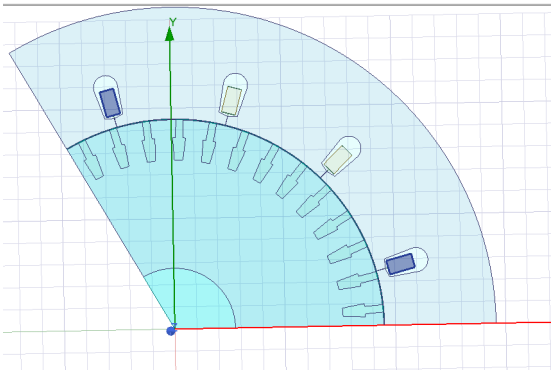

**Figure 4.5:** Position of the coil in the second examined case

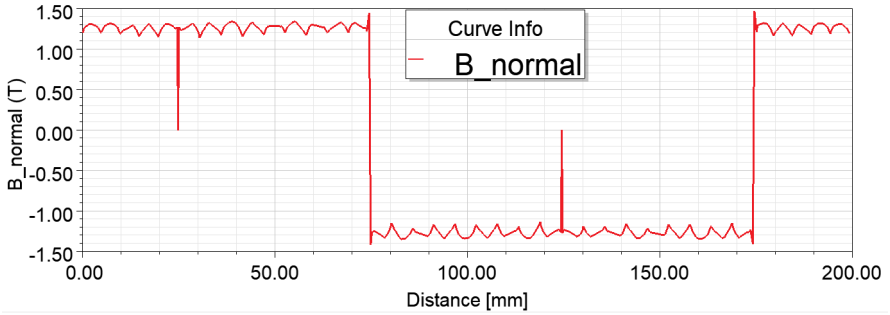


**Figure 4.6:** normal flux density across the stator surface for the first examined case

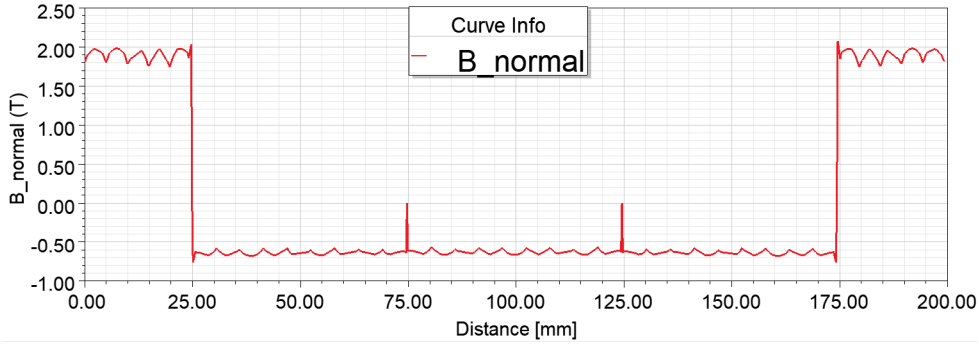


**Figure 4.7:** Normal flux density across the stator surface for the second examined case, here $A_{crossout}$ is 3 times smaller than $A_{crossin}$ resulting in that $B_{normalout}$ is 3 times bigger

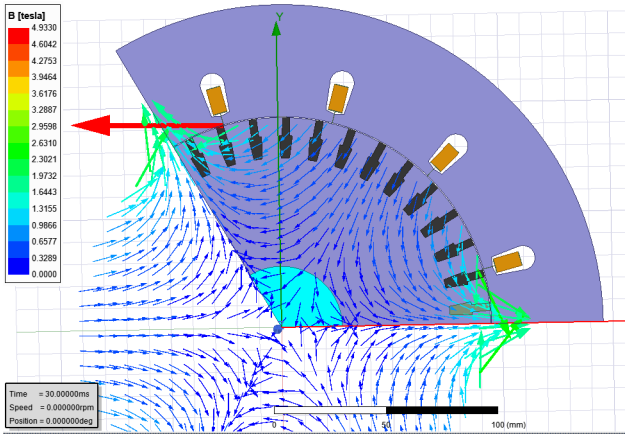


**Figure 4.8:** Normal flux density vectors in the area of the rotor for the second examined case

Now it is desired to find the inductance in the case of 3 coils excited by 3 phases. The modified version is shown in Figure 4.9.

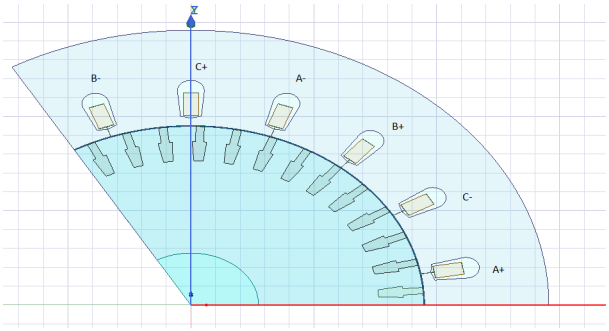


**Figure 4.9:** Modification with 3 coils and 3 phase excitation

First, the influence of one coil only as shown in Figure 4.10 will be studied. A simulation is performed with a current of 50A RMS, frequency of 50Hz and no rotor speed. The results are shown in Table 4.2

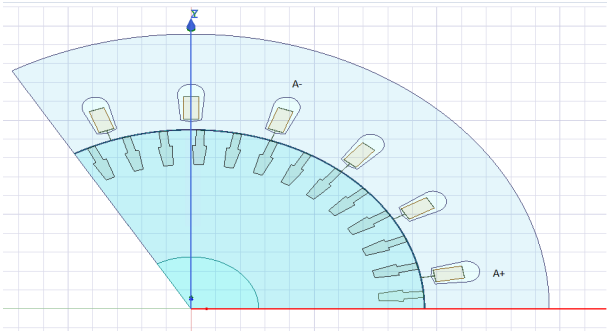


**Figure 4.10:** Examining the desired modification with the influence of only 1 coil.

In the case that the coil of phase $a$ is examined

$$A_{crossout} = A_{crossin} \tag{4.4}$$

According to (4.3) it is obtained

$$B_{normalin} = B_{normalout} \tag{4.5}$$

and the flux that flows between two slots, cause by phase $a$, can be expressed as

$$\Psi_{AA} = \frac{1}{3} B_{normalin} A_{crossin} = \frac{1}{3} \Psi_{coilA} \tag{4.6}$$

where
$\Psi_{AA}$ is the flux flowing between 2 slots caused only by the coil of phase $a$
$\Psi_{coilA}$ is the total flux of the coil of phase $a$

In the case of 3 coils excited by 3 phase currents as shown in Figure 4.9, it can similarly obtained that the flux that flows between two slots, cause by phase $b$ and $c$ can be expressed as

$$\Psi_{BB} = \frac{1}{3} \Psi_{coilB} \tag{4.7}$$

$$\Psi_{CC} = \frac{1}{3} \Psi_{coilC} \tag{4.8}$$

where
$\Psi_{BB}$ is the flux flowing between 2 slots caused only by the coil of phase $b$
$\Psi_{coilB}$ is the total flux of the coil of phase $b$
$\Psi_{CC}$ is the flux flowing between 2 slots caused only by the coil of phase $c$
$\Psi_{coilC}$ is the total flux of the coil of phase $c$

Table 4.2 shows the influence of phase $a$, phase $b$ and phase $c$ in all the teeth that are between the beginning and the end of the coil of phase $a$

**Table 4.2:** All fluxes that will build via superposition the total flux of phase $a$ in the case where all 3 coils are excited. MBA means the mutual flux between phase $b$ and phase $a$, while MCA means the mutual flux between phase $c$ and phase $a$.

| Fluxes from slot A+ to slot A- | | | |
|---|---|---|---|
| | tooth (slotx slotxx) | | |
| Flux type | A+ C- | C- B+ | B+ A- |
| Flux Phase A | $\Psi_{AA}$ | $\Psi_{AA}$ | $\Psi_{AA}$ |
| Flux MBA | -$\Psi_{BB}$ | -$\Psi_{BB}$ | $\Psi_{BB}$ |
| Flux MCA | $\Psi_{CC}$ | -$\Psi_{CC}$ | $-\Psi_{CC}$ |

Next step is to apply superposition and find the total flux of phase $a$. The flux of phase $a$ can be expressed as

$$\Psi A = 3\Psi_{AA} - 1\Psi_{BB} - 1\Psi_{CC} \tag{4.9}$$

Table 4.3 shows the results for the simulations Simulation 1 and Simulation 2. The two simulations are explained bellow

- Simulation 1 : Modification shown in Figure 4.10, current of 50A RMS, frequency of 50Hz and 38 number of turns
- Simulation 2: Modification shown in Figure 4.9, current of 50A RMS/phase, frequency of 50Hz and 38 number of turns

**Table 4.3:** Fluxes of phase $a$ for Simulation 1 and Simulation 2. In the case of Simulation 1 there is no contribution of phase $b$ or phase $c$. Therefore the calculated flux is the same with the flux taken from Ansys. The calculated flux comes from (4.9)

| Simulation | Fluxes | |
|---|---|---|
| | $\Psi_A$(Wb) from Ansys | $\Psi_A calculated$ (Wb) |
| Simulation 1 | 1.101104 | 1.101104 |
| Simulation 2 - | 1.4669 | 1.4681 |

The next step is to perform the flux calculation in the model shown in Figure 4.11. First, the influence of 1 coil only (see Figure 4.12) is examined. The total flux caused from 1 coil only is found to be 1.090834 Wb according to Ansys. Table 4.4 shows all the fluxes in all slots of phase A from all coils from all phases.

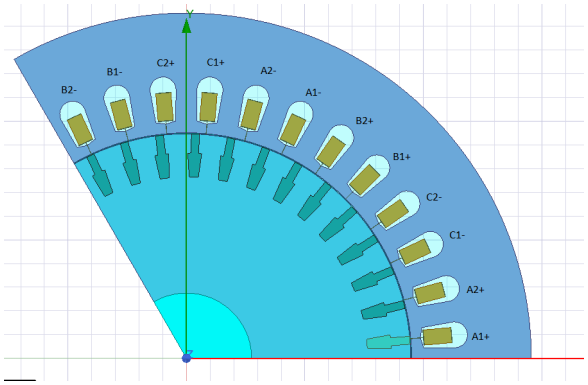


**Figure 4.11:** coils in the simulated IM 15kW

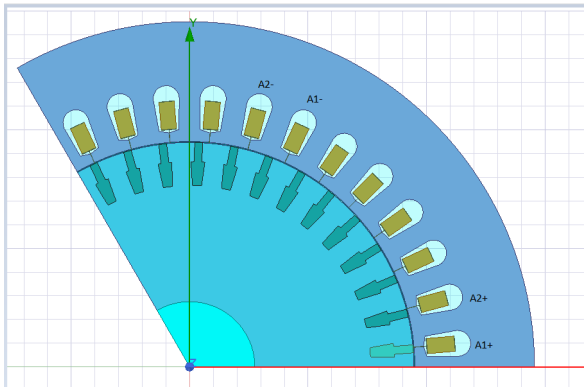


**Figure 4.12:** Examining only one coil of phase A

**Table 4.4:** All fluxes that will build via superposition the total flux of phase A

| Fluxes from A1+ to A2- | | | | | | | |
|---|---|---|---|---|---|---|---|
| flux type | tooth ( slotx slotxx) | | | | | | |
| | A1+ A2+ | A2+ C1- | C1- C2- | C2- B1+ | B1+ B2+ | B2+ A1- | A1- A2- |
| flux A1 | $\Psi_{AA}$ | $\Psi_{AA}$ | $\Psi_{AA}$ | $\Psi_{AA}$ | $\Psi_{AA}$ | $\Psi_{AA}$ | |
| flux A2 | | $\Psi_{AA}$ | $\Psi_{AA}$ | $\Psi_{AA}$ | $\Psi_{AA}$ | $\Psi_{AA}$ | $\Psi_{AA}$ |
| MA1A2 | | $\Psi_{AA}$ | $\Psi_{AA}$ | $\Psi_{AA}$ | $\Psi_{AA}$ | $\Psi_{AA}$ | -$\Psi_{AA}$ |
| MA2A1 | -$\Psi_{AA}$ | $\Psi_{AA}$ | $\Psi_{AA}$ | $\Psi_{AA}$ | $\Psi_{AA}$ | $\Psi_{AA}$ | |
| MC1A1 | $\Psi_{CC}$ | $\Psi_{CC}$ | -$\Psi_{CC}$ | -$\Psi_{CC}$ | -$\Psi_{CC}$ | -$\Psi_{CC}$ | |
| MC1A2 | | $\Psi_{CC}$ | -$\Psi_{CC}$ | -$\Psi_{CC}$ | -$\Psi_{CC}$ | -$\Psi_{CC}$ | -$\Psi_{CC}$ |
| MC2A1 | $\Psi_{CC}$ | $\Psi_{CC}$ | $\Psi_{CC}$ | -$\Psi_{CC}$ | - $\Psi_{CC}$ | -$\Psi_{CC}$ | |
| MC2A2 | | $\Psi_{CC}$ | $\Psi_{CC}$ | -$\Psi_{CC}$ | -$\Psi_{CC}$ | -$\Psi_{CC}$ | -$\Psi_{CC}$ |
| MB1A1 | - $\Psi_{BB}$ | -$\Psi_{BB}$ | -$\Psi_{BB}$ | -$\Psi_{BB}$ | $\Psi_{BB}$ | $\Psi_{BB}$ | |
| MB1A2 | | -$\Psi_{BB}$ | - $\Psi_{BB}$ | -$\Psi_{BB}$ | $\Psi_{BB}$ | $\Psi_{BB}$ | $\Psi_{BB}$ |
| MB2A1 | - $\Psi_{BB}$ | - $\Psi_{BB}$ | - $\Psi_{BB}$ | -$\Psi_{BB}$ | -$\Psi_{BB}$ | $\Psi_{BB}$ | |
| MB2A2 | | -$\Psi_{BB}$ | -$\Psi_{BB}$ | -$\Psi_{BB}$ | -$\Psi_{BB}$ | $\Psi_{BB}$ | $\Psi_{BB}$ |

Applying superposition it is obtained

$$\Psi_A = 20\Psi_{AA} - 8\Psi_{BB} - 8\Psi_{CC} \tag{4.10}$$

where
$fluxA1$ flux caused only from coil1 from phaseA
$fluxA2$ flux caused only from coil2 from phaseA
$MA1A2$ mutual flux caused by coil A1 to coil A2
$MA2A1$ mutual flux caused by coil A2 to coil A1
$MC1A1$ mutual flux caused by coil C1 to coil A1
$MC1A2$ mutual flux caused by coil C1 to coil A2
$MC2A1$ mutual flux caused by coil C2 to coil A1
$MC2A2$ mutual flux caused by coil C2 to coil A2
$MB1A1$ mutual flux caused by coil B1 to coil A1
$MB1A2$ mutual flux caused by coil B1 to coil A2
$MB2A1$ mutual flux caused by coil B2 to coil A1
$MB2A2$ mutual flux caused by coil B2 to coil A2

### 4.1.2 Finding Leakage Inductance

In the previous section, flux distribution was explained for different modified models. Leakage flux had been eliminated. In this section, leakage flux will be examined.

The initial slot opening is changed as shown in Figure 4.13. A part of the slot opening is made of air now which will allow a flux to flow. This flux will be the leakage flux. Rotor bars, like previously, are made of the same material as the core ($\mu$r of 100000). Figure 4.14 shows how the leakage flux will flow through the air in the slot opening.

Inductances can be calculated by hand if geometry and material are known. First, a magnetic circuit is made for the case of one coil as shown in Figure 4.15

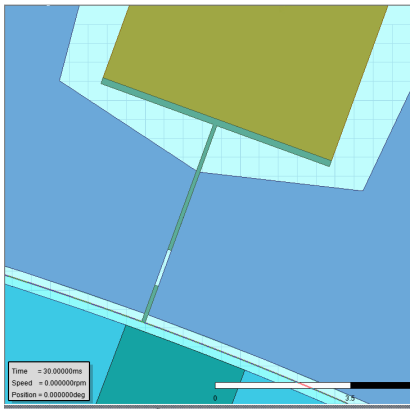

**Figure 4.13:** Modyfied slot opening, light green is the unreal material with $\mu r$ of 0.00001, one part of the slot opening is made of air with $\mu r$ of 1

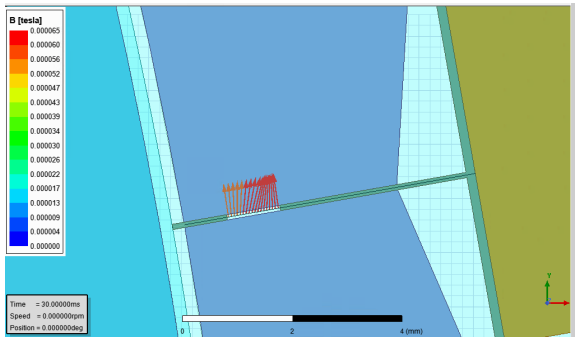

**Figure 4.14:** $B$ vector through the air in the slot opening

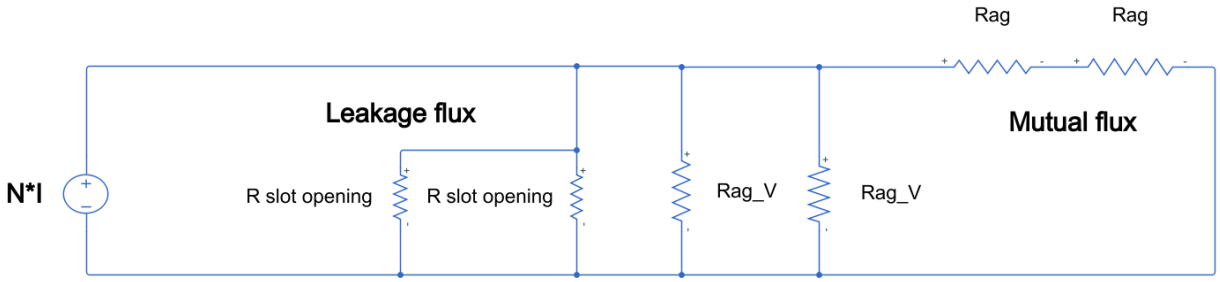


**Figure 4.15:** Magnetic circuit, relactances of the core material are neglected as the core material has $\mu r$ of 100000.

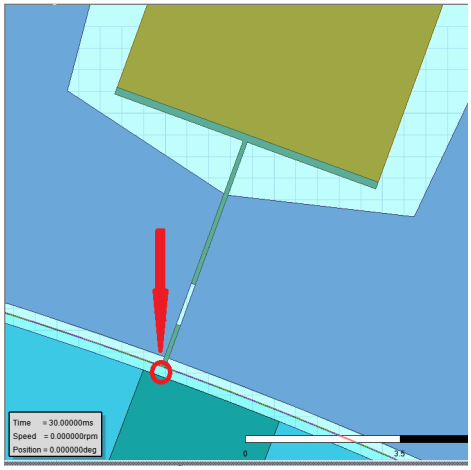


**Figure 4.16:** Position of the air gap which represents the reluctance $R_{agV}$

### Hand calculations

The reluctances of the circuit in Figure 4.15 are hand-calculated as

$$R_{ag} = \frac{L_{ag}}{L_{stack} Arc_{mean} \mu_0} \tag{4.11}$$

$$R_{agV} = \frac{w_{slot}}{L_{stack} L_{agV} \mu_0} \tag{4.12}$$

$$R_{slotopening} = \frac{w_{slot}}{L_{stack} L_{airopening} \mu_0} \tag{4.13}$$

where
$R_{ag}$ is the reluctance which represents the path of the flux as a normal component from the stator to the rotor through the air gap
$R_{slotopening}$ is the reluctance which represents the path of the leakage flux through the slot opening
$R_{agV}$ is the reluctance of the air-gap which is located between the end of the unreal material of the slot opening and the rotor. The part of this air gap is indicated in Figure 4.16
$L_{stack}$ is the stack length of the machine
$L_{ag}$ is the length of the air-gap
$Arc_{mean}$ is the mean length of the periphery of the cross section of $R_{ag}$
$w_{slot}$ is the width of the slot opening
$L_{agV}$ is the length of the path of $R_{agV}$
$L_{airopening}$ is the length of the cross section of $R_{slotopening}$
$\mu_0$ $4\pi \cdot 10^{-7}$

If we replace
$L_{stack} = 0.23m$,
$L_{ag} = 0.45mm$,

$Arc_{mean} = 99.4mm$,
$w_{slot} = 0.1mm$,
$L_{agV} = 0.23mm$,
$L_{airopening} = 1mm$,
then it is calculated that
$R_{ag} = 1.5671 \cdot 10^4 H^{-1}$,
$R_{slotopening} = 3.4599 \cdot 10^5 H^{-1}$,
and $R_{agV} = 1.5043 \cdot 10^6 H^{-1}$

It should be mentioned that $R_{agV}$ is very difficult to represent and en error is expected. However, an error in the value of $R_{agV}$ will not affect the calculation of slot leakage inductance.

First, a modified version with $Q$=18, $q$=1 and 1 excited coil as shown in Figure 4.9 will be examined. Leakage flux and mutual flux are defined from hand-calculations as

$$L_{mutual} = (\frac{N_{turns}^2}{2R_{ag}} + \frac{N_{turns}^2}{0.5R_{agV}})/N_{Pbranches} \tag{4.14}$$

$$L_{Leakage} = (\frac{N_{turns}^2}{0.5R_{slotopening}})/N_{Pbranches} \tag{4.15}$$

where
$L_{mutual}$ in this case is the inductance that represents the paths of $R_{agV}$ and $R_{ag}$
$L_{Leakage}$ is the inductance that represents the flux crossing the slot opening
$N_{Pbranches}$is the number of parallel branches per phase
$Q$ is the total number of slots
$q$ is the number of slots per pole per phase

For $N_{turns} = 38$ and $N_{Pbranches} = 3$, the mutual and leakage inductance become $L_{mutual} = 15.9975mH$ and $L_{Leakage} = 2.7824mH$

Table 4.5 shows the value of the Ansys output $L(phaseA, phaseA)$ (built in Ansys inductance calculator), the leakage and mutual inductances coming from the field analysis (using the Ansys field calculator), the self inductance coming from the division of the total flux (from Ansys result output) with the current (from Ansys result output) and the hand-calculated inductances for simulation of 1 coil excitation of 50A DC and no rotor speed.

**Table 4.5:** Inductance values. $L(phaseA, phaseA)$ comes from Ansys result output, $L_{mutual}field$ and $L_{Leakage}field$ come from the field analysis, $Ls$ $(\frac{\Psi}{i})$ comes from Ansys result output and $L_{Leakage}calculated$ and $L_{mutual}calculated$ are hand-calculated

| | Inductances | | | | | |
|---|---|---|---|---|---|---|
| | $L(phaseA, phaseA)$ | $L_{mutual}$ $field$ | $L_{mutual}$ $calculated$ | $L_{Leakage}$ $field$ | $L_{Leakage}$ $calculated$ | $Ls$ $(\frac{\Psi}{i})$ |
| Simulation of 50A DC, Q=18, q=1, 1 phase/-coil excited | 18.66mH | 15.884mH | 15.99mH | 2.768mH | 2.782mH | 18.66mH |

The case of $Q$=18, $q$=1 and 3 excited coils will be now examined. First, (2.37) and (4.9) are recalled, and the result becomes

$$\Psi_{TmainA} = 3\Psi_{AA} - 1\Psi_{BB} - 1\Psi_{CC} = \Psi_{mainA} - \frac{1}{3}(\Psi_{mainB} + \Psi_{mainC}) = (L_h + \frac{1}{3}L_h)i_{sa} \tag{4.16}$$

and it is also known that

$$\Psi_a = \Psi_{TmainA} + \Psi_{leakageA} = (\frac{4}{3}L_h + L_{leakage})i_{sa} \tag{4.17}$$

Combining (4.16) and (4.17), the total flux of phase $a$ can be expressed as

$$\Psi_a = L_h i_{sa} + 1/3 L_h i_{sa} + L_{leakage} i_{sa} = (L_h + L_{leakage})i_{sa} + M i_{sa} \tag{4.18}$$

and the mutual inductance between 2 phases can be expressed as

$$M = \frac{1}{3}L_h \tag{4.19}$$

where
$\Psi_{TmainA}$ is the total main flux of phase $a$
$\Psi_{leakageA}$ is the leakage flux of phase $a$
$\Psi_{mainA}$ is the main flux of a coil of phase $a$
$\Psi_{mainB}$ is the main flux of of a coil of phase $b$
$\Psi_{mainC}$ is the main flux of of a coil of phase $c$
$M$ is the mutual inductance between 2 phases
$L_h$ is the main inductance of phase $a$ caused only from the influence of phase $a$
$L_{leakage}$ is the leakage inductance of phase $a$, $b$ or $c$

It is reminded that in the examples where flux distribution was examined, leakage flux was eliminated which means that the flux of one phase was the main flux. Now the leakage inductance caused by leakage flux is added to the equation.

Table 4.6 shows the Ansys output $L(phaseA, phaseA)$, $L(phaseA, phaseB)$ (built in

Ansys inductance calculator), the hand-calculated leakage inductance and the self inductance coming from the division of stator flux with the stator current. $M_{average}$ represents the mean value of the Ansys outputs $L(phaseA, phaseB)$, $L(phaseA, phaseC)$ and $L(phaseC, phaseB)$.

**Table 4.6:** Inductances for case of $Q$=18, 1 excited phase with current of 50ADC.

| | Inductances | | | | |
|---|---|---|---|---|---|
| | $L(phaseA, phaseA)$ | $L(phaseA, phaseB)$ | $M_{average}$ | $L_{Leakage}\ hand-calculated$ | Ls $\frac{\Psi_A}{i_{sa}}$ |
| Simulation of 50A, f=50Hz, 3 excited coils, 0 rotor speed | 18.66mH | 5.2546mH | -5.288mH | 2.768mH | 23.94mH |

If it is assumed that the outputs from Ansys inductance matrix can be interpreted as

$$L(phaseA, phaseA) = L_h + L_{leakage} \tag{4.20}$$

and

$$L(phaseA, phaseB) = -M \tag{4.21}$$

then the self inductance can be expressed as

$$Ls = L(phaseA, phaseA) - L(phaseA, phaseB) \tag{4.22}$$

Using (4.22) for $Ls$ calculation an error of 0.0254mH is found, which corresponds to 0.1% error in $Ls$

It is also observed that $L(phaseA, phaseB)$, $L(phaseA, phaseC)$ and $L(phaseC, phaseB)$ have a very slightly different value, the reason of this deviation is unknown. Replacing $M$ with $M_{average}$, (4.22) gives an error of 0.008mH, which corresponds to 0.033% error in $Ls$. If the error is accepted then it can be concluded that

$$L(phaseA, phaseB) = -M \tag{4.23}$$

and

$$L(phaseA, phaseA) = L_h + L_{leakage} \tag{4.24}$$

According to (4.19) and (4.24), the leakage inductance $L_{leakage}$ is then calculated as

$$L_{leakage} = L(phaseA, phaseA) + 3L(phaseA, phaseB) \tag{4.25}$$

The leakage inductance that is calculated according to (4.25) is 2.796mH which gives an error of 1.01% in the estimation of leakage inductance.

With the same strategy as before, the case of $Q$=36, $q$=2 with the same materials as before is examined. From (4.23) and (4.10) the mutual inductance can be expressed as

$$M = -L(phaseA, phaseB) = \frac{8}{20}L_h \tag{4.26}$$

and combining (4.23), (4.23) and (4.26) the leakage inductance can be expressed as

$$L_{leakage} = L(phaseA, phaseA) + \frac{20}{8}L(phaseA, phaseB) \tag{4.27}$$

Table 4.7 shows the calculated leakage inductance from field analysis (using Ansys field calculator), the total leakage inductance from hand-calculation (the number of stator slots are different now) and the two Ansys output inductances (built in Ansys inductance calculator) for the simulation of 50A RMS current and 50Hz.

**Table 4.7:** Inductances from Ansys result output, hand-calculated leakage inductance and leakage inductance from the field analysis (using Ansys field calculator)

| | Inductances | | | |
|---|---|---|---|---|
| | $L(phaseA, phaseA)$ | $L(phaseA, phaseB)$ | $L_{leakage}$calculated | $L_{leakage}$from field analysis |
| Simulation of 50A, $f$=50Hz, 3 excited coils, $Q$=36 and $q$=2 | 58.124mH | -21.207mH | 5.1065mH | 5.52mH |

### 4.1.3 Adding saturation

Figure 4.17 shows how the inductances will oscillate in case of a non-linear core material. The model of $Q$=18, $q$=1 will be used for the simulations. The stator slot modification is the same as in the previous chapter.

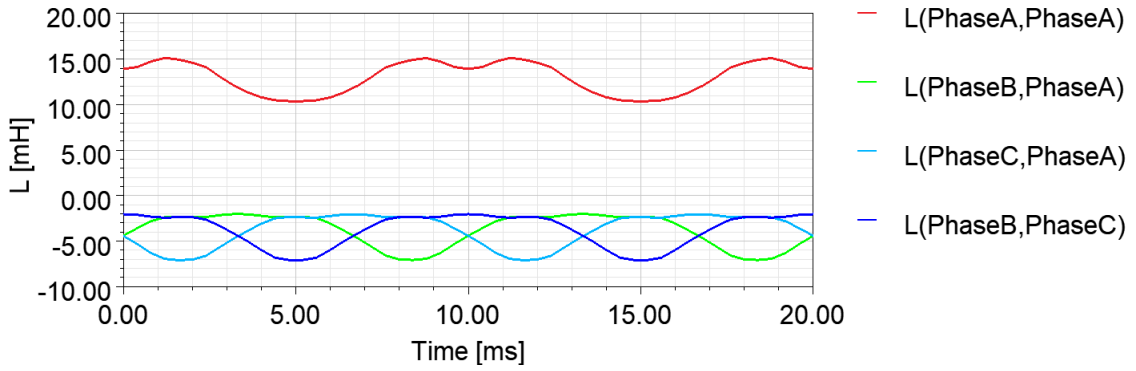


**Figure 4.17:** Indactances from Asnys output data when non-linear M700 core material is used. Model of $Q$=18, $q$=1 and 3 excited coils where used with excitation of 50A RMS and 50Hz

According to [10] the component of the 2nd harmonic of the mutual inductance is also contributing to the fundamental flux. Considering the second harmonic of the inductances the equation for the self inductance calculation can be expressed as

$$Ls = LAA_{DC} + M_{DC} - LAA_2 - M_2 \tag{4.28}$$

If the 2nd harmonic is not taken into account then the self inductance is expressed as

$$Ls = LAA_{DC} + M_{DC} \tag{4.29}$$

and the leakage inductance is expressed as

$$Lsl = LAA_{DC} - 3M_{DC} \tag{4.30}$$

where
$LAA$ is the sum of the main inductance of phase $a$ and the stator leakage inductance of phase $a$
$M$ is the the mutual inductance between 2 phases
$LAA_{DC}$ is the mean value of $LAA$
$M_{DC}$ is the mean value of $M$
$LAA_2$ is the second harmonic magnitude of LAA
$M_2$ is the second harmonic magnitude of M
$Lsl$ is the leakage stator inductance of one phase

It should be noted that the calculation of leakage inductance has been made only according to (4.30)

Simulations with a current sweep from 5A to 45A RMS at 50Hz and no rotor speed

have been made. More specifically, the following simulations have been made:

- Simulation 1: linear core material, no rotor bars
- Simulation 2: steel M700 core material, no rotor bars
- Simulation 3: steel M700 core material, aluminium rotor bars without eddy effect in them
- Simulation 4: steel M700 core material, no rotor bars and the special flux blocker material covers all the volume of the stator slot opening so leakage inductance is eliminated

Figure 4.18 shows the leakage inductance (for Simulation 1, Simulation 2 and Simulation 4) by means of calculation according to (4.30) and the measured leakage inductance from the field analysis. It is observed that (4.30) is not giving very good estimation of leakage inductance in the cases of M700 as core material.

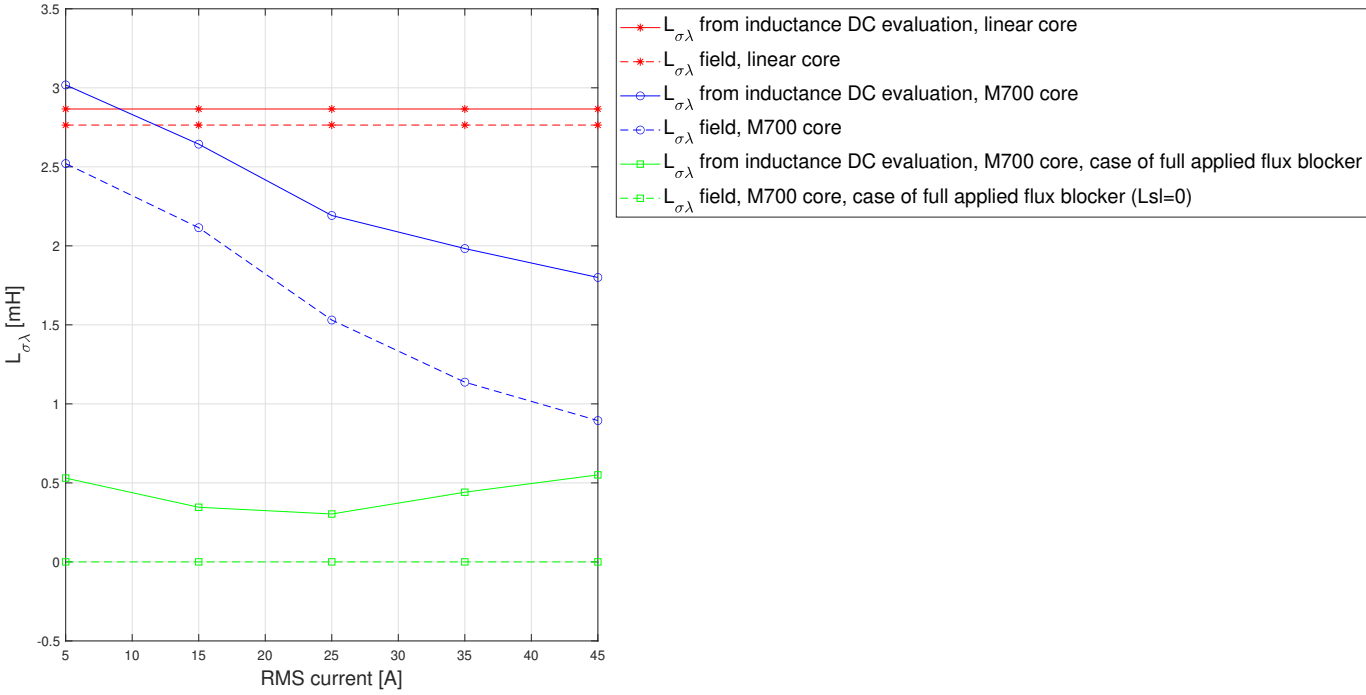


**Figure 4.18:** Comparison of calculated leakage inductance according to (4.30) and the leakage inductance measured from the field analysis (from Ansys field calculator)

Figure 4.19 shows the calculated self inductance using (4.28), (4.29) and the one that comes from $\Psi a/ia$, where $\Psi a$ and $ia$ are taken from the Ansys result output.

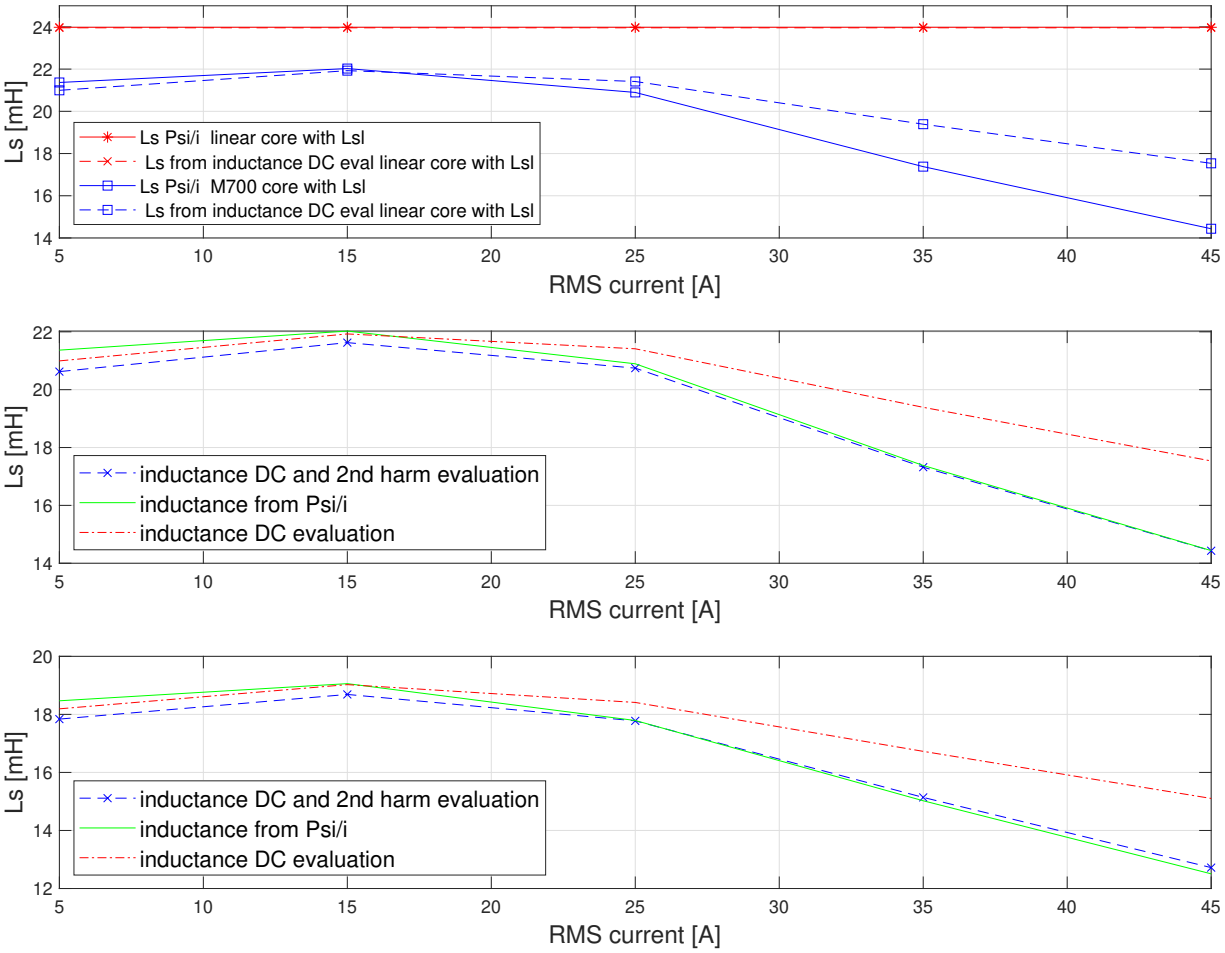


**Figure 4.19:** Upper plot: self inductance calculated from (4.29) and $\Psi a/ia$ for the cases of Simulation 1 and Simulation 2. Middle plot: self inductance calculated from (4.28) (blue dash line), (4.29) (red dash-dot line with cross) and $\Psi a/ia$ (green solid line) for the cases of Simulation 2. Lower plot: self inductance calculated from (4.28) (blue dash line), (4.29) (red dash-dot line with cross) and $\Psi a/ia$ (green solid line) for the cases of Simulation 2.

### Testing equations in IM at no load

It is desired to see what results the equations (4.28) and (4.29) will give in case of calculating self inductance at no load operation. Now, the model is the initial IM machine with $Q$=36, $q$=2, core material of M700 and rotor bars made of aluminium. No load simulations at 50Hz, 1000rpm and a current sweep from 5A to 40A RMS are made. In Figure 4.20 is shown the self inductance estimated from $\Psi a/ia$ (coming from the Ansys result output) and the self inductance calculated from (4.28) and (4.29) (making use of the inductances built in Ansys inductance calculator).

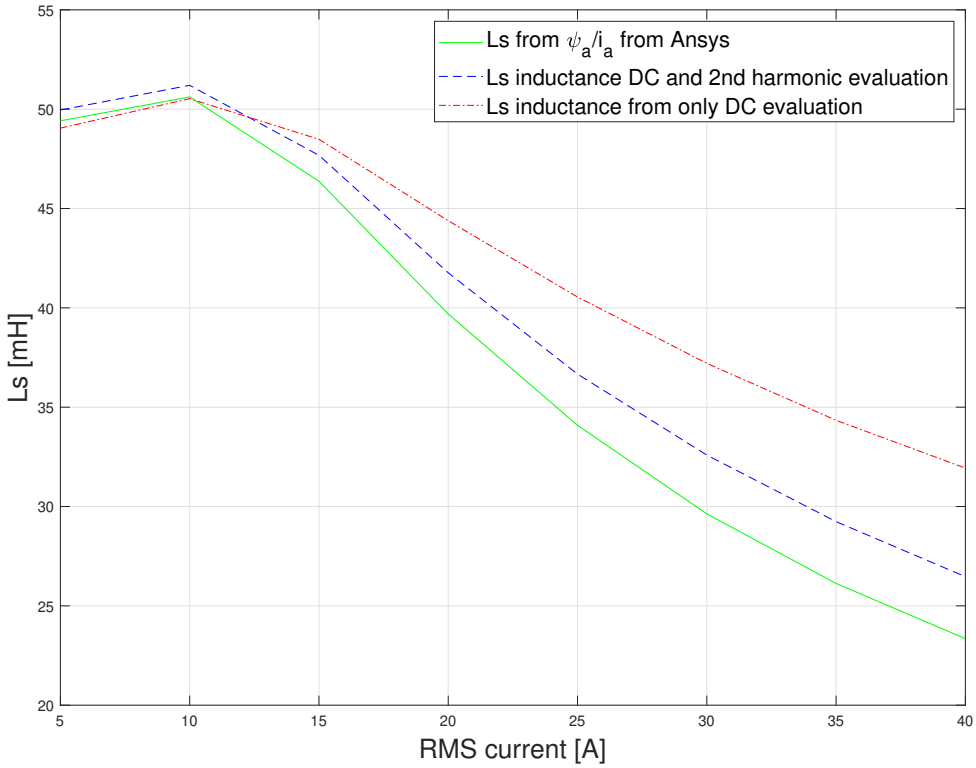


**Figure 4.20:** Solid green line: self inductance calculated from Ansys outputs $\psi a$, $ia$. Blue dash line: self inductance calculated from 4.28. Red dash-dot line: self inductance calculated from 4.29

Figure 4.21 shows the flux of the phase $a$ from Ansys and the one obtained using (2.37) for the no load simulation at 40A RMS. It is observed that (2.37) does not reflect to the flux with a great precision. The reason for this is unknown.

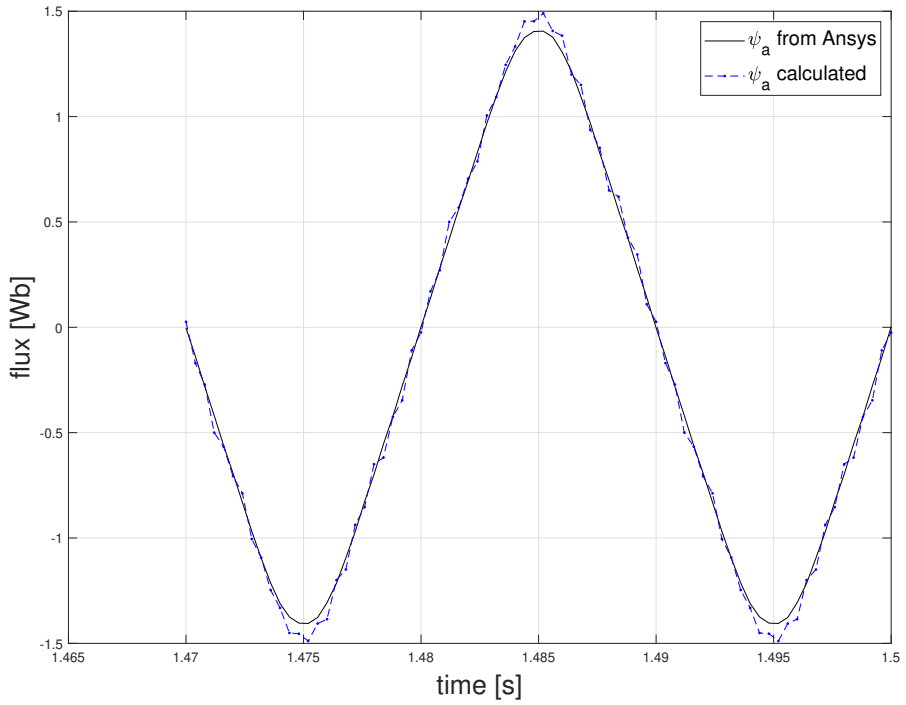


**Figure 4.21:** Black solid line: flux of phase a from Ansys result output. Blue dash-dot line: calculated flux using 2.37 (making use of the inductances built in Ansys inductance calculator)

## 4.2 Power balance check

A power unbalance have been observed after processing Ansys output data. This causes an error to the flux, torque and voltage equations we may use for parameter identification.

Induced voltage is an output from Ansys simulation which is calculated from Ansys by differentiate the flux,

$$e_a = \frac{d\psi_a}{T_{step}} \tag{4.31}$$

where
$e_a$ is the induced voltage of phase a
$\psi_a$ is the flux of phase a
$T_{step}$ is the time step

That means that $e_a$ will be delayed by half of a time step. A phase correction of $e_a$ will lead re-express $e_a$ as

$$e_{anew} =\mid e_{aold} \mid e^{j(\theta_{old}+\theta_{correction})} \tag{4.32}$$

where:
$e_{aold}$ is the induced voltage before the correction
$e_{anew}$ is the induced voltage after the correction
$\theta_{old}$ is the angle of induced voltage before the correction
and

$$\theta_{correction} = 0.5\frac{T_{step}}{T}2\pi \tag{4.33}$$

where $T$ is the period

**Power balance at locked rotor test**

It is desired to see how the correction angle from (4.33) will correct the power balance in the locked rotor test. A locked rotor test is carried out at frequency of 10Hz and a current sweep from 10 to 30A RMS. Table 4.8 shows the power missing in case of not using the correction angle. Table 4.9 shows the power balance in case of using the correction angle.

**Power balance at load test**

**Table 4.8:** Discrepancy in power balance in case of not correcting the induce voltage

| Power balance at locked rotor without corrected angle | | | | | |
|---|---|---|---|---|---|
| Current sweep | 10A RMS | 15A RMS | 20A RMS | 25ARMS | 30A RMS |
| Discrepancy | 4.2W | 9.6W | 17.1W | 26.8W | 38.5W |

**Table 4.9:** Discrepancy in power balance in case of correcting the induced voltage.

| Power balance at locked rotor with corrected angle | | | | | |
|---|---|---|---|---|---|
| Current sweep | 10ARMS | 15ARMS | 20ARMS | 25ARMS | 30ARMS |
| Discrepancy | 0.30W | 0.69W | 1.25W | 1.95W | 2.80W |

Power balance is not satisfied in case of a load test even if (4.33) is used. The exact reason for this is unknown.

In case of a load test torque unbalance is observed between the Torque from Ansys output and the calculated electromagnetic torque (see(2.5)). This torque unbalance could be a possible reason for the power unbalance that is observed for the case of a load test.

Three simulation with voltage excitation at 220V RMS, 50Hz and slip frequency of 0.5Hz, 1Hz and 1.5Hz are made. Table 4.10 shows the torque from Ansys and the calculated electromagnetic torque for the three operation points. Table 4.11 shows the error in the power balance for the three operation points. It is noted that in the equation of power balance the torque from Ansys is used and not the electromagnetic calculated torque.

**Table 4.10:** Comparison between torque from Ansys and the calculated electromagnetic torque ($T_e$ stands for the calculated electromagnetic torque)

| Torque comparison in Voltage excitation of 220V RMS and 50Hz | | | |
|---|---|---|---|
| slip frequency | 0.5Hz | 1Hz | 1.5Hz |
| $T_e$ calculated | 89.2787Nm | 166.7245Nm | 240.2055Nm |
| Torque Ansys | 88.3027Nm | 164.7277Nm | 236.9517Nm |
| Discrepancy | 0.976Nm | 1.9968Nm | 3.2538Nm |

**Table 4.11:** Power balance for the three operation points. Power in is the input electrical power, Power out stands for mechanical output power, Power loss stands for the total losses, Discrepancy stands for the unbalance between the Power in and the summation of the mechanical output power and total losses. The calculation of the output mechanical power uses the torque from Ansys and not the electromagnetic calculated torque

| Power balance in Voltage excitation of 220V RMS and 50Hz | | | |
|---|---|---|---|
| slip frequency | 0.5Hz | 1Hz | 1.5Hz |
| Power in | 9492.7W | 17785.3W | 25770W |
| Power out | 9150.4W | 16905.2W | 24080W |
| Power loss | 358.5W | 890.7W | 1722.7W |
| Discrepancy | 16.14W | 10.65W | 32.97W |

**Torque calculation from field analysis**

Some efforts have been made in order to calculated the torque from field analysis. First, the Maxwell stress tensor needs to be calculated,

$$s = \frac{B_t B_n}{\mu 0} - \frac{B_{mag}^2}{2\mu 0}\delta_{tn} \tag{4.34}$$

where
$s$ is the Maxwell stress tensor
$B_t$ is the tangential component of B vector
$B_n$ is the normal component of B vector
$\mu 0$ $4\pi 10^{-7}$
$B_{mag}$ is the magnitude of B vector
$\delta$ is the Kronecker's delta.

In the case where only the tangential force is needed the second term is ignored. The Maxwell stress tensor equation is simplified

$$s = \frac{B_t B_n}{\mu 0} \tag{4.35}$$

The line which was used in order to sample the points of interest for the calculation of the Maxwell stress tensor was taken according to Figure 4.22.

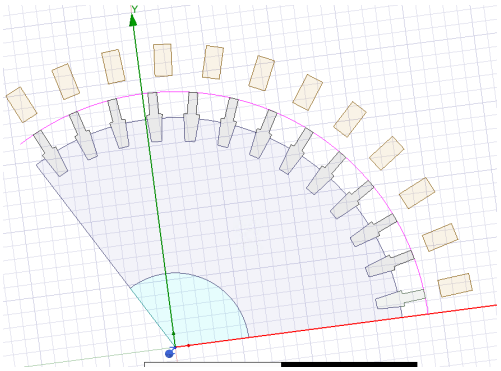

**Figure 4.22:** Used line (purple) to sample the B vector in order to calculate the Maxwell stress tensor. Some parts of the machine like a part of the rotor and the stator are hidden in order to make the line more visible

The torque can be expressed with the Maxwell stress tensor and the geometry of the machine as

$$Torque = s_{average} A_{outer} r_{rotor} \tag{4.36}$$

where:
$s_{average}$ is the average stress across the line
$A_{outer}$ is the outer surface of the rotor (outer periphery times stack length)
$r_{rotor}$ is the radius of rotor

The simulation of voltage excitation at 220V RMS, frequency of 50Hz and speed of 980rpm will be examined. Figure 4.23 shows the torque that Ansys provides as output and the calculated torque according to (4.36) and sampling according to Figure 4.22. Moreover, Figure 4.23 shows the calculated torque using an extra smooth operator in Ansys field calculation. The position of this operator is shown in Figure 4.24.

Table 4.12 shows the average torque coming from Ansys result output, the average calculated torque according to (4.36) and the average calculated torque using an extra smooth operator in Ansys field calculation.

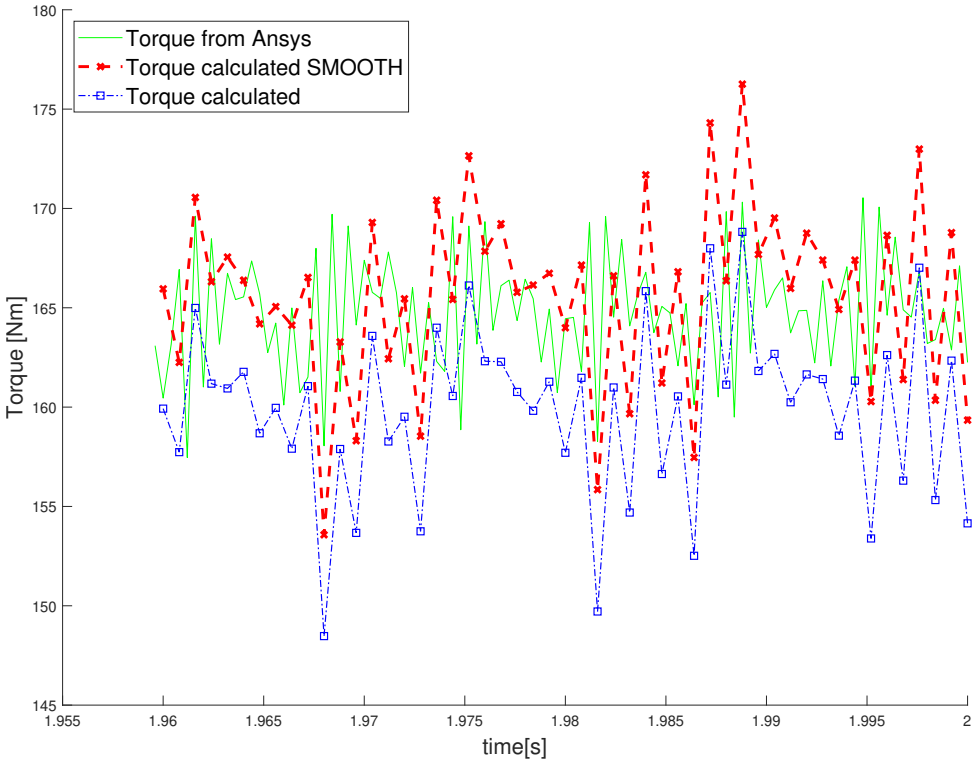


**Figure 4.23:** Green solid line: Torque from Ansys. Blue dashed-dot line: calculated torque. Red dashed line: calculated torque using the smooth operator

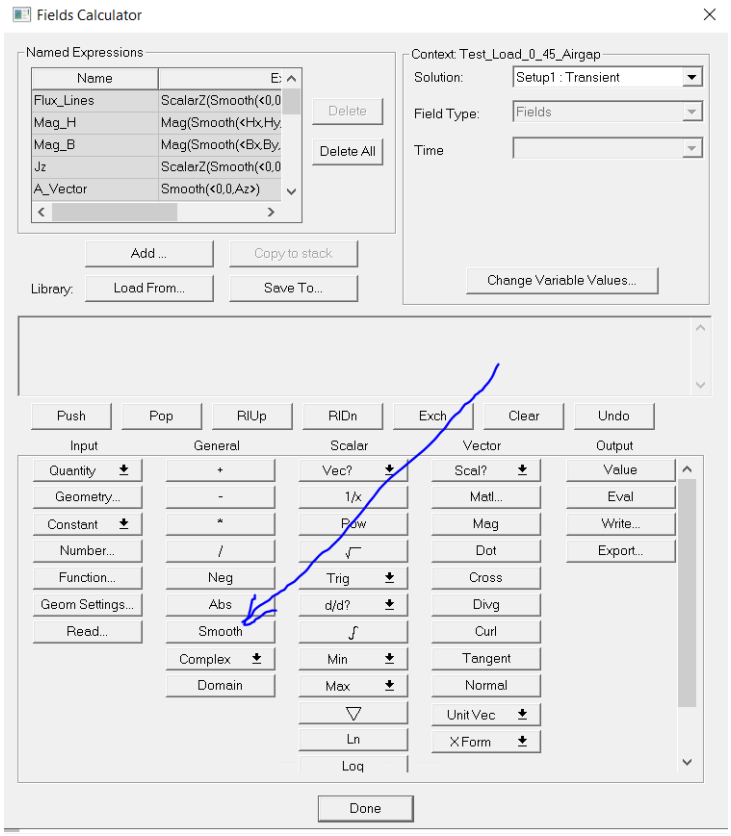


**Figure 4.24:** Position of smooth operator in Ansys field calculator

**Table 4.12:** Average value of the torque for 220V RMS, 50Hz and 980rpm. $Torque_{Ansys}$ stands for the average torque coming from Ansys result output. $Torque_{calculated}$ stands for the average torque that is calculated according to (4.36). $Torque_{smooth}$ stands for the average torque that is calculated according to (4.36) but using the smooth operator from Ansys field calculator

| Torque kind | value |
|---|---|
| $Torque_{Ansys}$ | 164.7111Nm |
| $Torque_{calculated}$ | 159.8686Nm |
| $Torque_{smooth}$ | 165.5841Nm |

## 4.3 Rotor resistance

In this chapter an estimation of rotor resistance is made. The rotor resistance is estimated from a locked rotor test and from field analysis.

Moreover, the rotor resistance can be calculated considering the material and geometry dimensions. Equations (2.47), (2.48), (2.54) are recalled, giving

$$\rho_{al} = 28.2 \cdot 10^{-9} \cdot (1 + 4.3 \cdot 10^{-3} \cdot (T_{al} - 20)) \tag{4.37}$$

$$R_{bar} = \rho_{al} L_a / A_{bar} \tag{4.38}$$

where
$T_{al}$ is the temperature of the aluminium in Celcius
$L_a$ is the length of the bar
$A_{bar}$ is the cross section of the bar in the case of current in z direction

Considering the temperature inside the aluminium to be 30, the resistivity of aluminium is found to be $2.9413 \cdot 10^{-8} m$. However, in this project a resistivity of $3.0252 \cdot 10^{-8} m$ is used. In addition, the cross section of the rotor bar $A_{bar}$ is measured from Ansys and is found to be $76.41786574 \cdot 10^{-6} m^2$. The stack length $L_A$ is $0.23m$. Therefore (4.38) gives a value of $9.1052 \cdot 10^{-5}$ which is the resistance of one rotor bar.

The coefficient to connect the rotor equivalent resistance to stator equivalent is calculated according to (2.51) which is recalled

$$coef_{reqS} = \frac{3 n_s^2 q_s^2 k_1^2 poles^2}{Q_r c_s^2} \tag{4.39}$$

where
$Q_r$ is the number of total bars
$poles$ is the number of total poles
$n_s$ is the number of turns per coil
$q_s$ is the number of slots per phase per pole pair
$k_1$ is the harmonic winding factor
$c_s$ is the winding factor which depends on the way the phases are connected and the parallel branches

If $Q_r = 38$, $poles = 6$, $n_s = 38$, $q_s = 1$, $c_s = 3$ and $k_1 = 0.9659$, then $coef_{reqS} = 1.6582 \cdot 10^3$. The stator equivalent rotor resistance is calculated as

$$R_r = R_{bar} coef_{reqS} = 0.1509799 \qquad (\Omega) \tag{4.40}$$

It should be noted that the end ring is not modelled in the simulations.

### 4.3.1 Rotor resistance from locked rotor test

Some efforts have been made in order to calculate the rotor resistance from the locked rotor test. Simulations have been carried out at 10Hz, 0rpm and a current sweep from 10 to 30 A RMS. It should be noted that in case of current excitation Ansys does not consider the stator resistance

Two approaches have been made. One using $\tau$ model and one approach using $\urcorner$ model.

#### $\tau$ model approach

Figure 4.25 shows the simplified equivalent circuit used for the calculation of rotor resistance. The value of mutual inductance is unknown and difficult to estimate. Therefore an aproximation between the stator current and the rotor current is made

$$\hat{i_r} = 0.95\hat{i_s} \tag{4.41}$$

The rotor resistance is calculated from

$$R_r = \frac{P_{solid}}{\frac{3}{2}\hat{i_r}^2} \tag{4.42}$$

where
$R_r$ rotor resistance in $\tau$ model
$\hat{i_r}$ is the pick of the fundamental of the rotor current
$\hat{i_s}$ is the pick of the fundamental of the stator rotor current
$P_{solid}$ is the average solid losses taken from Ansys result output

Figure 4.26 shows the results of $R_r$ according to (4.42)

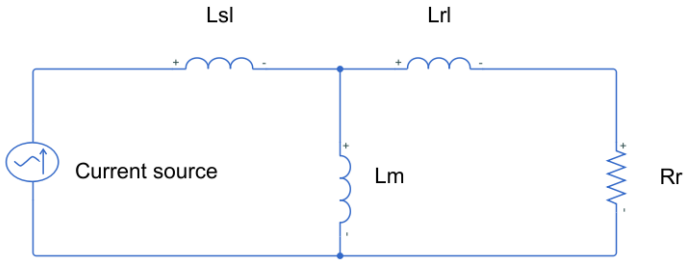


**Figure 4.25:** simplified $\tau$ circuit for the case of current excitation

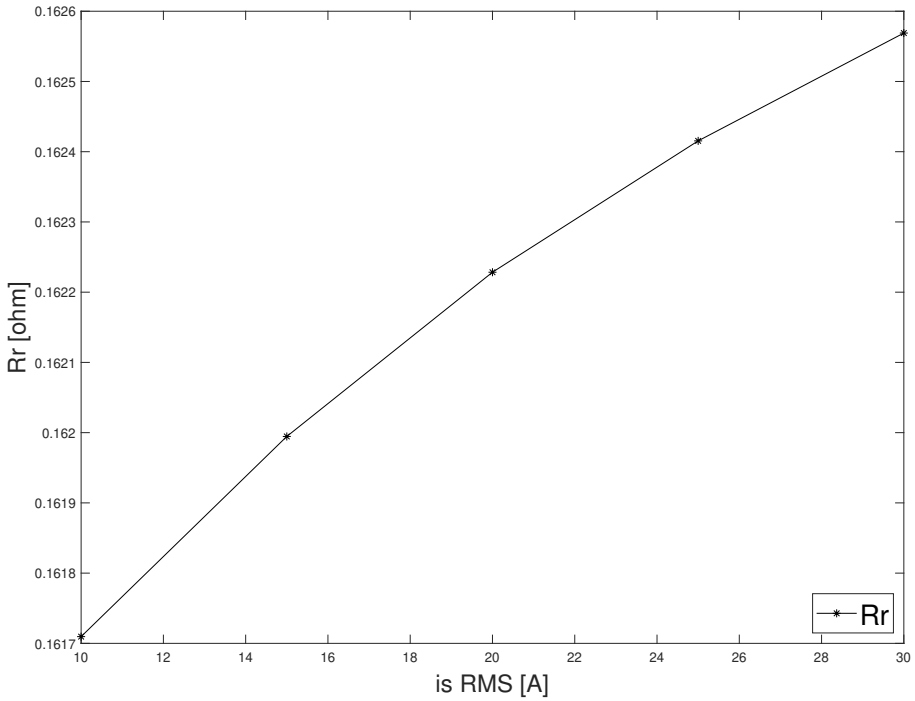


**Figure 4.26:** $R_r$ calculated according to (4.42) for a current sweep of 10-30A RMS

### ⅂ model approach

Figure 4.27 shows the ⅂ model. Now the resistance of the rotor in ⅂ model will be estimated. It should be noted that in case of current excitation Ansys does not consider the stator resistance

The total impedance of the circuit of Figure 4.27 is

$$Z_{circuit} = Z_{Lsigna} + Z_{LM}//R_R \tag{4.43}$$

$Z_{circuit}$ is the total impedance from the circuit
$Z_{Lsigna}$ is the impedance of the leakage inductance in ⅂ model
$Z_{LM}$ is the impedance of magnetization inductance
$R_R$ is the rotor resistance in ⅂ model

The total impedance can be also expressed from the relation between stator voltage and stator current

$$Z_{ei} = \frac{e_s}{i_s} \tag{4.44}$$

where
$Z_{ei}$ is the total impedance from the ratio of voltage over current

$e_s$ is the induced voltage
$i_s$ is the stator current

Setting (4.43) and (4.44) equal, it is obtained that

$$\Re Z_{circuit} = \Re Z_{ei} \tag{4.45}$$

and

$$\Re Z_{LM}//RR = \Re Z_{ei} \tag{4.46}$$

$$\Im Z_{circuit} = \Im Z_{ei} \tag{4.47}$$

$R_R$ is a part of $Z_{LM}//R_R$ which does not include the leakage inductance $L_{sigma}$. Therefore, the unknowns are $R_R$ and $Z_{LM}$. $R_R$ can be estimated if a sweep of $L_M$ values is made. Figure 4.28 shows the potential values of $R_R$ during a sweep of $L_M$ values. In this way an approximation of $R_R$ is made. If $R_R$ is known, then an approximation of $L_{sigma}$ can be made. Figure 4.29 shows the possible values of $L_{sigma}$ during a sweep of $L_M$

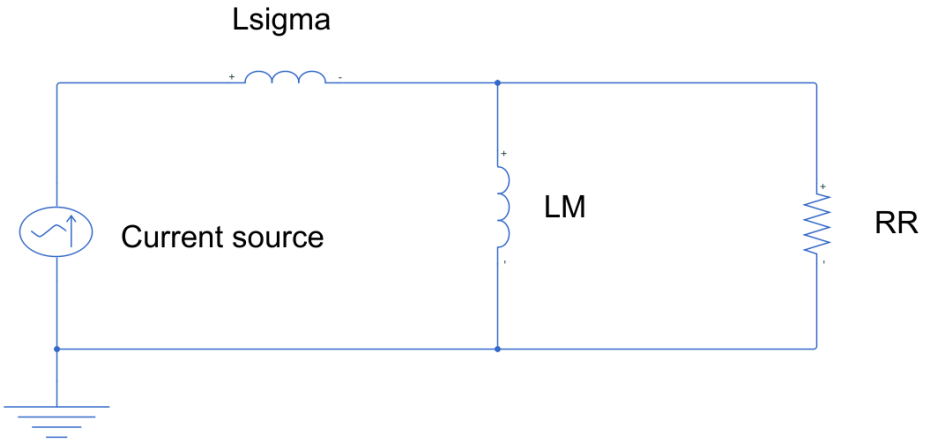


**Figure 4.27:** circuit of ⅂ model

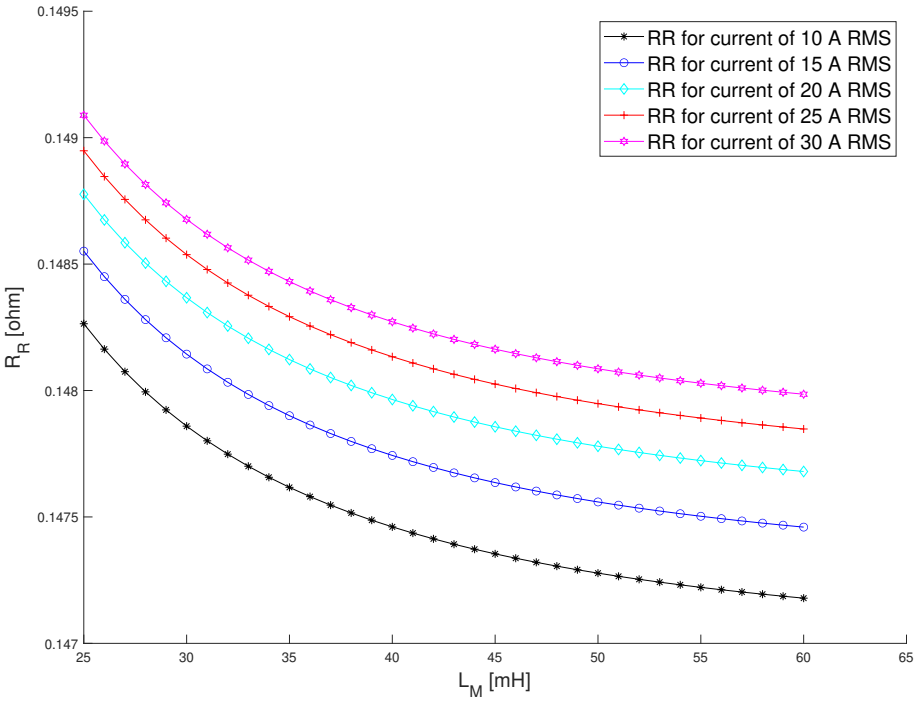


**Figure 4.28:** $R_R$ values at locked rotor test during a sweep of $L_M$.

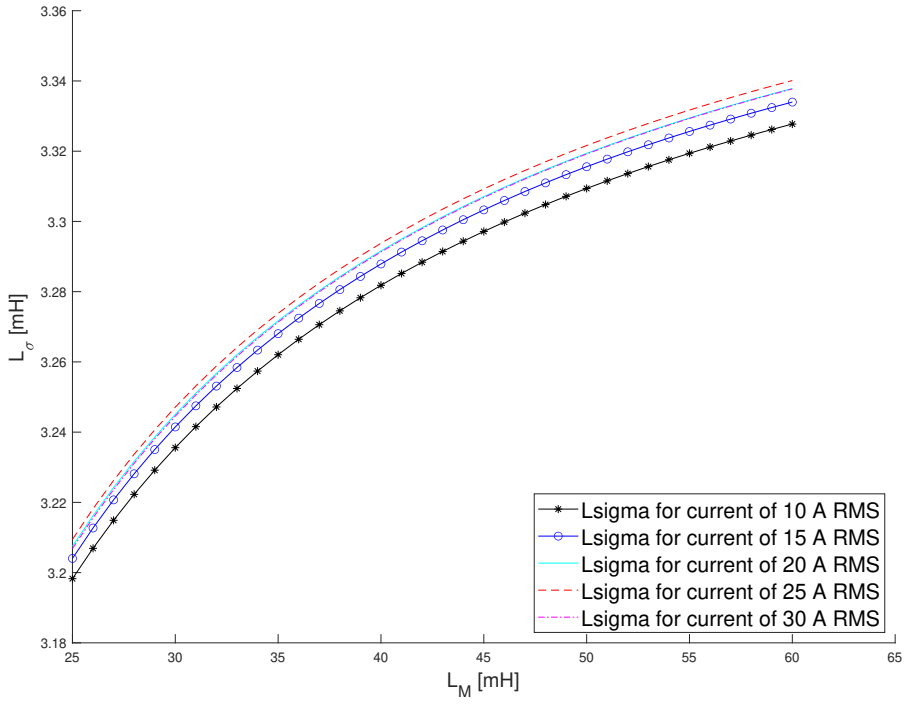


**Figure 4.29:** $L_{sigma}$ values at locked rotor test during a sweep of $L_M$.

### 4.3.2 Rotor resistance from field analysis

Some efforts have been made in order to estimate the rotor resistance from field analysis at load simulation.

First, let us begin with the torque equation in the DQ frame

$$T_e = \frac{3n_p}{2}\Psi_R iq \tag{4.48}$$

It is known from the theory that

$$\Psi_R = b\psi r \tag{4.49}$$

and

$$i_R = \frac{i_r}{b} \tag{4.50}$$

Equations (4.50) and (4.49) give

$$\Psi_R i_R = \psi_r i_r \tag{4.51}$$

In addition, it is known from the theory that the rotor current can be expressed as

$$i_r R_r = \psi r w_{slip} \tag{4.52}$$

$$i_r = \psi r w_{slip}/Rr \tag{4.53}$$

Combining (4.48), (4.51) and (4.53), $R_r$ can be expressed in terms of $T_e$ and $i_r$

$$R_r = \frac{T_e}{\frac{n_p \cdot 3/2 \cdot i_r^2}{w_{slip}}} \tag{4.54}$$

where
$T_e$ is the electromagnetic torque
$n_p$ is the number of pole pairs
$i_r$ is the rotor current in $\tau$ model

$w_{slip}$ is the slip angular speed
$R_r$ is the Rotor resistance in $\tau$ model
$\psi_r$ is the rotor flux in $\tau$ model
$\Psi_R$ is the rotor flux in $\urcorner$ model
$i_R$ is the rotor current in $\urcorner$ model
$b$ is the important ratio constant

The rotor current was taken from the field analysis. Figure 4.30 shows the current in the z direction of a rotor bar for the simulation of voltage excitation at 220V RMS, 50Hz and slip frequency of 1Hz. This current is the rotor bar current in the rotor side. In order to obtain the equivalent rotor current at the stator side, coefficient according to (2.51) is used

$$i_r = i_{rr} coef_{ieqS} \tag{4.55}$$

where
$i_{rr}$ is the rotor current in the rotor side
$i_r$ is the funtametal of the rotor current in the stator side
$coef_{ieqS}$ is the coefficient to connect the rotor equivalent current to stator equivalent

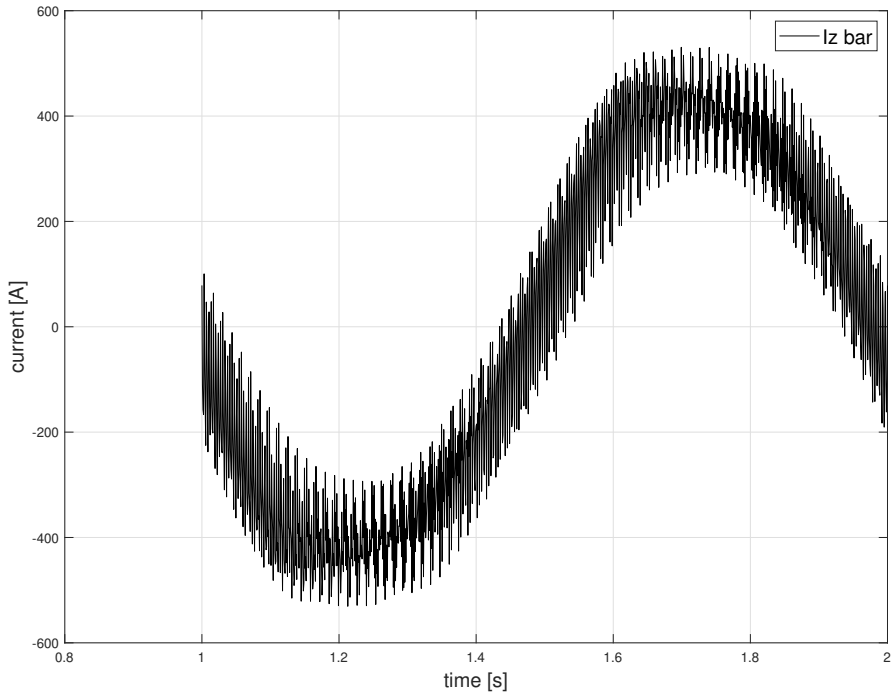


**Figure 4.30:** Rotor current in the rotor side for the simulation of 220V RMS, 50Hz and 1Hz of slip frequency. The time of sampling is 1 second which is the slip period of the rotor current

Four simulation have been made with voltage excitation of 220V RMS, 50Hz and a slip frequency of 1, 1.5, 2, and 2.5 Hz. Table 4.13 shows the rotor resistance

according to (4.54) using rotor current from field sampling.

**Table 4.13:** $T_e$ was calculated according to (2.5), $i_r$ is the stator equivalent rotor current (the fundamental component) from the field analysis and $R_r$ is calculated according to (4.54)

| Voltage excitation 220V RMS, 50Hz and 3 slip frequency points | | | | |
|---|---|---|---|---|
| slip frequency | 1Hz | 1.5Hz | 2Hz | 2.5Hz |
| $i_r$ | 39.1998 A | 57.954 A | 76.0441 A | 93.4207 A |
| $R_r$ | 0.15156 ohm | 0.15167 ohm | 0.15156 ohm | 0.15168 ohm |
| $T_e$ | 166.7973 Nm | 243.2201 Nm | 313.8533 Nm | 379.2279 Nm |

## 4.4 Stator leakage inductance

In this chapter stator leakage inductance is approximated. The material of the core is changed to a steel with constant relative permeability of 100000. In this way the effect of saturation will not affect the simulation. Two approaches have been made

**Approach 1: No load test**

In this approach, the leakage inductance is estimated from a no load test using the Ansys inductance matrix. If a linear core material is used then Ansys inductance matrix can be useful as shown in chapter 4.1. A no load test is been carried out at frequency of 50Hz, rotor speed of 1000rpm and phase current of 32 A RMS. Table 4.14 shows the Ansys outputs $L(PhaseA, PhaseA)$, $L(PhaseA, PhaseB)$ and the calculated inductance from (4.27)

**Table 4.14:** Calculation of leakage inductance $L_{\sigma\lambda}$ calculated from no load test and using the data from Ansys inductance matrix and the equations from flux distribution (see(4.27 ))

| Simulation | $L(PhaseA, PhaseA)$ | $L(PhaseA, PhaseB)$ | $L_{\sigma\lambda}$ calculated |
|---|---|---|---|
| No load simulation at 32A RMS, 50Hz and 1000rpm rotor speed | 39.458mH | 15.5363mH | 0.617mH |

**Approach 2: Making the rotor a flux blocker**

In this approach the rotor has been replaced by an unreal material with relative permeability of 0.00001. In this way all the flux is flowing from the paths of the leakage inductance. A simulation has been made at a current of 32A RMS and frequency of 50Hz. Table 4.15 shows the the Ansys outputs $L(PhaseA, PhaseA)$, $L(PhaseA, PhaseB)$, the calculated inductance from (4.27) and the calculated self inductance from the division of $\psi_a/i_a$ ($\psi_a$ and $i_a$ are taken from Ansys result output).

The leakage inductances that were calculated by approach 1 and approach 2 are not identical. However, the value is small and in case of approach 1 an error would affect the value of the estimated leakage inductance a lot.

**Table 4.15:** Calculation of leakage inductance in the case of replacing the rotor with the material of very low permeability. All the flux is in principle the measured leakage flux which gives the leakage inductance

| Simulation | $L(PhaseA, PhaseA)$ | $L(PhaseA, PhaseB)$ | $L_{\sigma\lambda}$ calculated | $L_s$ $(\psi_a/i_a)$ |
|---|---|---|---|---|
| Simulation at 32A RMS, 50Hz | 0.8482mH | 16nH | 0.8482mH | 0.8482mH |

## 4.5 Parameter estimation

In this chapter a parameter estimation will be described.

### 4.5.1 Processing the data

The inputs used for the parameter estimation in this chapter are

- $\psi_s$ : the fundamental component of the stator flux (taken from Ansys result output) in xy coordinates
- $i_s$ : the fundamental component of the stator current (taken from Ansys result output) in xy coordinates
- $\omega_{slip}$ : the slip angular speed
- $\hat{i_r}$ : the magnitude of the stator equivalent rotor current from the field analysis (see (4.55) )
- $b$ : the important ratio constant (see (2.6)). A guess of $b$ is made in order to estimate the possible parameters.

If the rotor leakage inductance $L_{r\lambda}$ is expressed as a ratio $a$ of the mutual inductance $L_m$, then the important ratio constant $b$ can be expressed as

$$L_{r\lambda} = aL_m \tag{4.56}$$

$$b = \frac{L_m}{L_m + L_{rl}} = \frac{L_m}{L_m + aL_m} = \frac{1}{1+a} \tag{4.57}$$

and in this case a guess of $b$ means a guess of $a$.

First, the electromagnetic torque $T_e$ is estimated from

$$T_e = 3\frac{n_p}{2}\Im\psi_s^* i_s \tag{4.58}$$

After that, the rotor resistance in the $\tau$ model $R_r$ is estimated from

$$R_r = \frac{T_e}{\frac{n_p \cdot 3/2 \cdot i_r^2}{w_{slip}}} \tag{4.59}$$

and the rotor resistance in the ⅂ model can be estimated from

$$R_R = b^2 R_r \tag{4.60}$$

The rotor flux $\Psi_R$ in the ⅂ model can be calculated now from

$$T_e = \frac{3n_p}{2} \frac{\Psi_R^2}{R_R} w_{slip} \tag{4.61}$$

$$\Psi_R = \sqrt{\frac{T_e R_R}{\frac{3n_p}{2} w_{slip}}} \tag{4.62}$$

The current $iq$ in the ⅂ model is estimated from

$$i_q = \Psi_R \omega_{slip} / R_R \tag{4.63}$$

and the current $id$ in the ⅂ model is found from

$$i_d = \sqrt{\hat{i_s}^2 - i_q^2} \tag{4.64}$$

Moreover, the magnetizing inductance $L_M$ in the ⅂ model and the mutual inductance $L_m$ in the $\tau$ model can be estimated from

$$L_M = \Psi_R / i_d \tag{4.65}$$

$$L_M = \frac{L_m^2}{L_m + L_{r\lambda}} = b L_m \tag{4.66}$$

Now the angle $dq$ is known which means that the stator flux $\psi_s$ can be expressed in $dq$ coordinates ($\psi_{Sdq}$) as

$$\psi_{Sdq} = \psi_{Sd} + j\psi_{Sq} \tag{4.67}$$

The leakage inductance $L_\sigma$ can be estimated from

$$\psi_{Sdq} = \psi_R + i_{dq} L_\sigma \tag{4.68}$$

$$L_\sigma = \psi_{Sq} / i_q \tag{4.69}$$

Furthermore, the leakage inductance of the stator $L_{\sigma\lambda}$ (in the $\tau$ model) can be estimated from the approximation of $L_\sigma$ as

$$L_\sigma = L_{r\lambda} + L_{\sigma\lambda} = aL_m + L_{\sigma\lambda} \tag{4.70}$$

$$L_{\sigma\lambda} = L_\sigma - L_{r\lambda} \tag{4.71}$$

Figure 4.31 shows the process of parameter calculation in short.

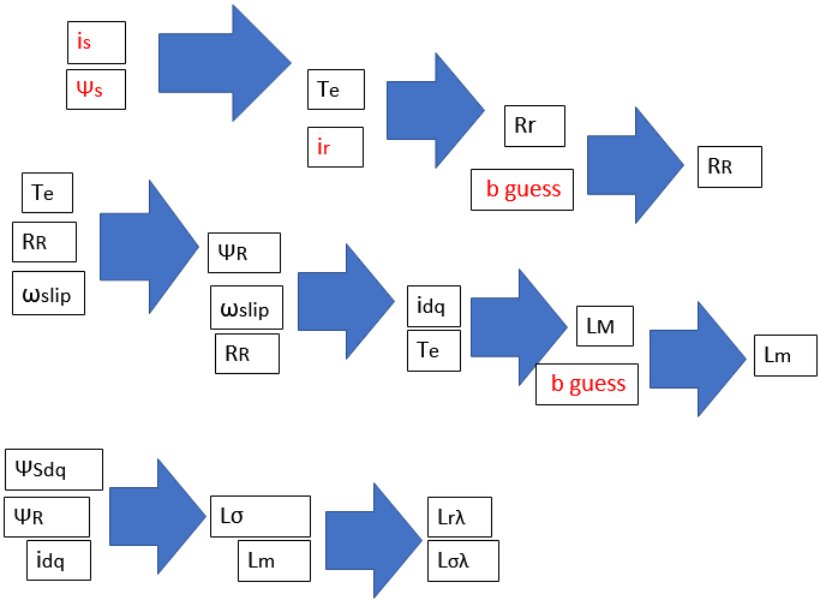


**Figure 4.31:** Parameter calculation process. The inputs are colored with red letters

### 4.5.2 Results at load test

The simulations of voltage excitation of 220V RMS, 50Hz and slip frequency of 1Hz, 1.5Hz, 2Hz and 2.5Hz will be examined. 5 guessed of $b$ are made as follow

- guess 1: the rotor leakage inductance $L_{r\lambda}$ is 1% of the mutual inductance $L_m$

- guess 2: the rotor leakage inductance $L_{r\lambda}$ is 2% of the mutual inductance $L_m$
- guess 3: the rotor leakage inductance $L_{r\lambda}$ is 3% of the mutual inductance $L_m$
- guess 4: the rotor leakage inductance $L_{r\lambda}$ is 4% of the mutual inductance $L_m$
- guess 5: the rotor leakage inductance $L_{r\lambda}$ is 5% of the mutual inductance $L_m$

Figure 4.32 shows the estimated parameters $L_M$,$R_R$ and $L_\sigma$ of the ⅂ model

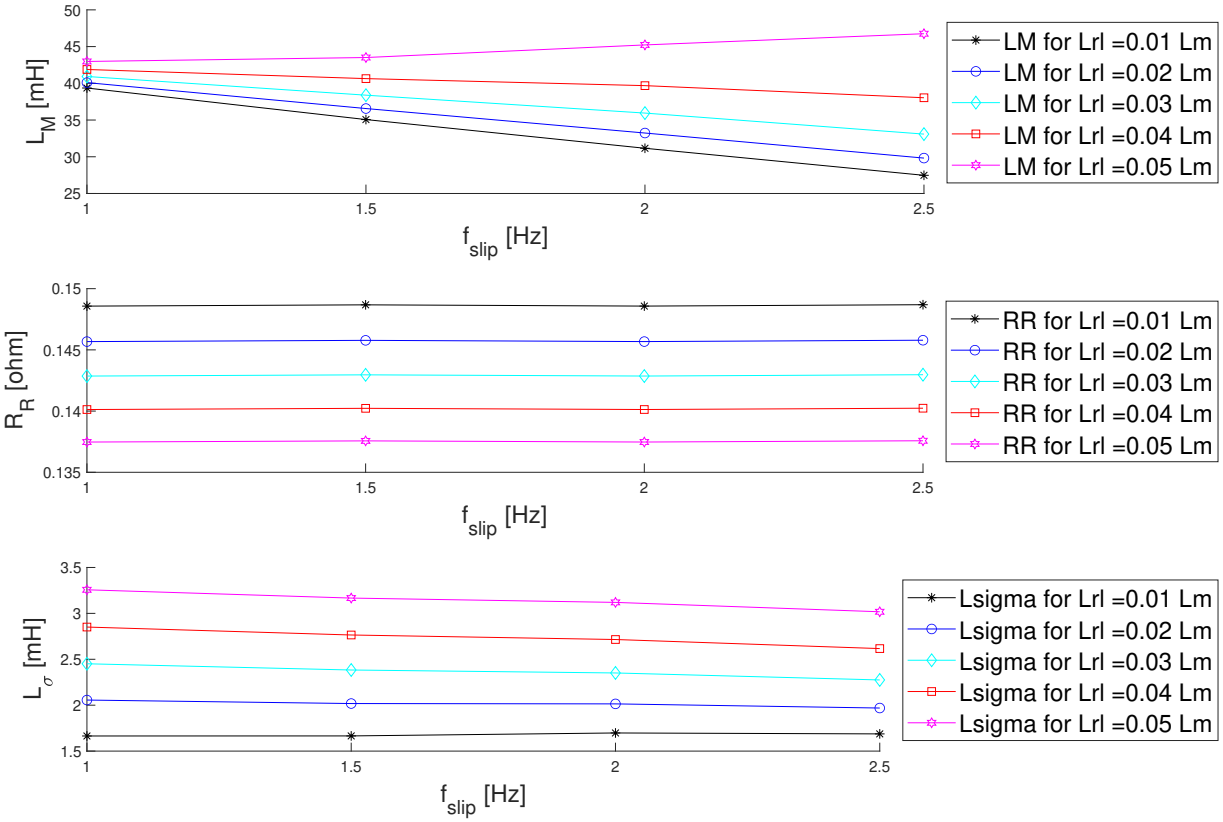


**Figure 4.32:** Parameter estimation in the ⅂ model. Upper plot: magnetizing inductance $L_M$ for all 5 guesses of $b$. Middle plot: rotor resistance $R_R$ for all 5 guesses of $b$. Lower plot: leakage inductance $L_{sigma}$ for all 5 guesses of $b$.

Figure 4.33 shows the estimated parameters $L_{\sigma\lambda}$, $R_R$ and $L_{r\lambda}$ of the $\tau$ model

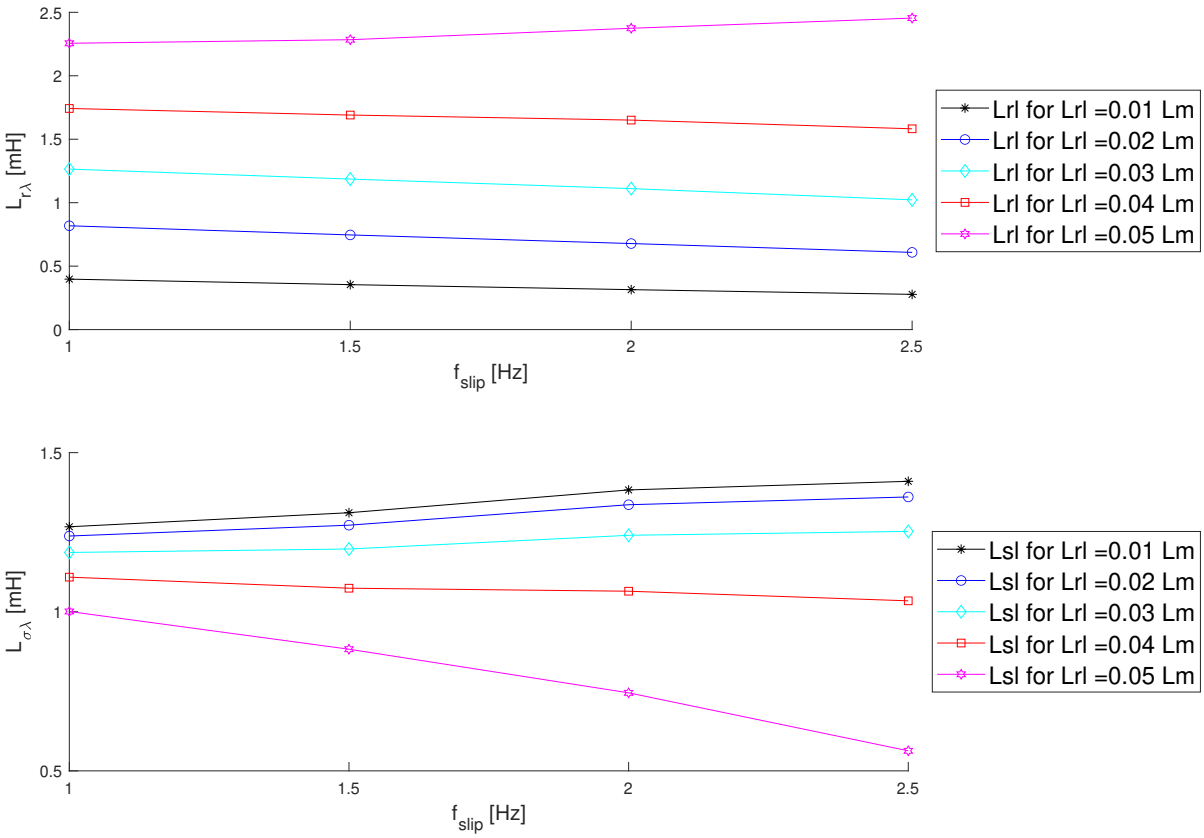


**Figure 4.33:** Parameter estimation in the $\tau$ model. Upper plot: stator leakage inductance $L_{\sigma\lambda}$ for all 5 guesses of $b$. Lower plot: rotor leakage inductance $L_{r\lambda}$ for all 5 guesses of $b$.

Figure 4.32 (lower plot) shows the possible values of $L_\sigma$. Possible values of $L_\sigma$ have been also obtained from the locked rotor test (see Figure 4.29 ). $L_\sigma$ from the locked rotor test is around 3.25mH. That value would match in Figure 4.32 (lower plot of $L_\sigma$) when $L_{r\lambda}$ is around 5% of $L_m$.

Figure 4.32 (middle plot) shows the possible values of $R_R$. Possible values of $R_R$ have been also obtained from the locked rotor test (see Figure 4.28 ). $R_R$ from the locked rotor test is around 0.148ohm. That value would match in Figure 4.32 (middle plot of $R_R$) when $L_{r\lambda}$ is around 1% of $L_m$. However, this value is considered to be too low.

Comparing the parameters $R_R$ and $L_\sigma$ between the locked rotor test and the load test gives different matches. The exactly reason for this is unknown. One possible reason is that the rotor resistance in locked rotor test is expected to be a little higher (locked rotor test is been carried out at 10Hz).

## 4.6 Sustainable aspects

United Nations established 17 sustainable goals in 2015. Two of these goals are related to this project.

- Infrastructure and Industrialization: investigating the parameters of an induction machine could help to understand better the induction machine and use cheaper materials. That would make the induction machine a more attractive option for industrial applications.

- Climate change: acquiring a better accuracy for the parameters of the induction machine could help the design of an effective controller. An effective controller increases the efficiency of the induction machine and decreases the losses of the induction machine (which are actually heat to environment).

# 5

# Conclusion and future work

## 5.1 Conclusion

Investigating the influence of the output inductance matrix from Ansys gave good results in the case of a linear core material. Flux distribution was examined in chapter 4.1 and the derived equations made sense when they were combined with Ansys inductance matrix only for the case of linear material in the core. In the cases of non linear material in the core, the equations coming from the flux distribution were not satisfied. The exact reason is unknown. One more approach to re-express the equations was made with the inclusion of the second harmonic of the inductances. However, the result did not help to understand the behaviour of the inductances in saturated material. According to the investigation of this paper, the inductance matrix from Ansys can be useful for computing the stator leakage inductance and the self inductance in the case of non saturated material.

The power balance from the Ansys data processing was examined in chapter 4.2. Correcting the phase of the induced voltage gave a better power balance in the case of a locked rotor test. However, in the case of a load test, the power balance was not satisfied. The exact reason for this is unknown. One reason that is believed to influence the power balance is the unbalance between the electromagnetic torque (which can be calculated from theoretical equations) and the output torque given by Ansys. A manual calculation of the torque had been carried out. The results gave a close approach of the rotor moving torque, compared with the torque from Ansys.

The rotor resistance estimated from the field analysis gave very close results compared with the rotor resistance obtained by theoretical calculations.

An approximation of the stator leakage inductance was made in chapter 4.4. However, the results were not encouraging and more investigation is needed.

Parameter estimation has been described in chapter 4.5 in the case of a load test. An estimation of possible values of the parameters in the $\Gamma$ model and in the $\tau$ model has been carried out.

## 5.2 Future work

Utilizing the inductance matrix from Ansys in the case of saturation needs further investigation. The equations coming from the flux distribution were not satisfied when the material of the core was changed to a non linear material.

More ways to estimate the parameters of an induction machine would give a better feeling about the accuracy of the parameters in the $\tau$ and in the $\urcorner$ model. Moreover, the sensitivity of the rotor resistance estimation needs to be examined.

# Bibliography


[1] Tuovinen, T., Hinkkanen, M., Luomi, J. (2010). Modeling of saturation due to main and leakage flux interaction in induction machines. IEEE Transactions on industry applications, 46(3), 937-945.

[2] Thiringer, T. (1996). Measurements and modelling of low-frequency disturbances in induction machines (Doctoral dissertation, Chalmers University of Technology).

[3] Roshanfekr Fard, P. (2013). Energy-efficient generating system for HVDC offshore wind turbine.

[4] Krings, A., Nategh, S., Stening, A., Grop, H., Wallmark, O., Soulard, J. (2012). Measurement and modeling of iron losses in electrical machines. In 5th International Conference Magnetism and Metallurgy WMM'12, June 20th to 22nd, 2012, Ghent, Belgium (pp. 101-119). Gent University.

[5] Wallmark, O. (2014). AC machine analysis-fundamental theory. KTH Royal Institute of Technology.

[6] Luomi, J. (1998). Transient phenomena in electrical machines. Chalmers University, Sweden.

[7] Harnefors, L. (2002). Control of variable-speed drives. Applied Signal Processing and Control, Department of Electronics, Mälardalen University.

[8] Kylander, G. (1995). Thermal modelling of small cage induction motors. Chalmers University of Technology.

[9] SÁNCHEZ, E. G., SARANGI, T. A. Simulation of an Induction Machine for Electric Vehicle Purpose.

[10] J. Ruan and S. Wang, "Magnetizing Curve Estimation of Induction Motors in Single-Phase Magnetization Mode Considering Differential Inductance Effect," in IEEE Transactions on Power Electronics, vol. 31, no. 1, pp. 497-506

[11] Wikipedia, "Maxwell stress tensor" `https://en.wikipedia.org/wiki/Maxwell_stress_tensor`

[12] Klaes, N. R. (1993). Parameter identification of an induction machine with regard to dependencies on saturation. IEEE Transactions on Industry Applications, 29(6), 1135-1140.

[13] Chiver, O., Micu, E., Barz, C. (2008, May). Stator winding leakage inductances determination using finite elements method. In 2008 11th International Conference on Optimization of Electrical and Electronic Equipment (pp. 69-74). IEEE.